Pharmaceutical Sciences and Drug Design
ISSN: 3062-4428
2022, Volume 2, Page No: 245-264
Copyright CC BY-NC-SA 4.0
Available online at: www.galaxypub.co/page/journals

Galaxy Publication

Galaxy Publication

Design, Synthesis, and Activity of Triazole-Based Molecular Hybrids with Antistaphylococcal Properties

Emily J. Parker[1]*, Olivia S. Grant[1], Thomas K. Reed[1], Michael D. Harris[1]

[1]Department of Drug Development, School of Pharmacy, University of Nottingham, Nottingham, United Kingdom.

***E-mail** ✉ emily.parker@gmail.com

Received: 26 May 2022; **Revised:** 14 August 2022; **Accepted:** 16 August 2022

ABSTRACT

In the context of increasing antibiotic resistance, the development of novel small molecules exhibiting selective, narrow-spectrum inhibition of bacterial-specific enzymes or proteins—with high potency and reduced adverse effects—represents a key priority in drug discovery. Accordingly, we established and executed a successful methodology for identifying new hybrid structures, particularly the relatively underexplored [2-(3-R-1H-1,2,4-triazol-5-yl)phenyl]amine derivatives. These scaffolds function as modular platforms, facilitating the attachment of specific functional groups to improve activity against staphylococcal pathogens. The desired compounds were synthesized through streamlined single-reaction protocols, utilizing transformations of suitably substituted 4-hydrazinoquinazolines or 2-aminobenzonitrile starting materials in combination with appropriate carboxylic acid reagents. Putative interactions as DNA gyrase inhibitors were examined via computational docking simulations, supporting their assessment for antistaphylococcal potential. A considerable number of the prepared analogs demonstrated strong inhibitory activity toward Staphylococcus aureus (MIC values: 10.1–62.4 μM). In particular, 5-bromo-2-[3-(furan-3-yl)-1H-1,2,4-triazol-5-yl]aniline and 5-fluoro-2-[3-(thiophen-3-yl)-1H-1,2,4-triazol-5-yl]aniline displayed MICs of 5.2 μM and 6.1 μM, respectively, nearly matching the reference compound ciprofloxacin (MIC: 4.7 μM). Structure-activity relationship (SAR) studies and ADME predictions highlight opportunities for further optimization. The [2-(3-R-1H-1,2,4-triazol-5-yl)phenyl]amine series exhibits notable antimicrobial efficacy and justifies advanced exploration as targeted antistaphylococcal therapeutics. SAR findings emphasize that cycloalkyl or electron-rich heterocyclic groups at the triazole 3-position are critical for activity, whereas methylation of the aniline ring increases potency. Halogen incorporation into the aniline ring produces mixed effects, varying with the triazole 3-substituent. The synthesized [2-(3-R-1H-1,2,4-triazol-5-yl)phenyl]amines show substantial antistaphylococcal effects and warrant in-depth investigation as promising antibacterial candidates.

Keywords: Triazole, «one-pot» synthesis, Molecular docking, Antistaphylococcal activity.

How to Cite This Article: Parker EJ, Grant OS, Reed TK, Harris MD. Design, Synthesis, and Activity of Triazole-Based Molecular Hybrids with Antistaphylococcal Properties. Pharm Sci Drug Des. 2022;2:245-64. https://doi.org/10.51847/qwGKIVwLY6

Introduction

Although antibiotic treatments have advanced considerably, the susceptibility of pathogens to available antimicrobial agents continues to decline progressively over time, leading to the rise of resistant bacterial strains in both community-acquired and nosocomial infections. This trend stems from the restricted range of efficacious therapeutic options for managing infectious diseases [1, 2], compounded by inappropriate and excessive application of these agents, which promotes the development of combined established and novel resistance pathways [3, 4].

Particularly alarming are infections triggered by Staphylococcus aureus, owing largely to its extensive array of virulence elements, such as toxins, superantigens, and membrane-associated exoproteins. Moreover, the appearance of methicillin-resistant Staphylococcus aureus (MRSA) isolates in hospital environments and among the general population has heightened infection risks, as these organisms typically exhibit resistance to multiple

© 2022 Pharmaceutical Sciences and Drug Design

drug classes. Consequently, this poses severe clinical challenges, including elevated patient morbidity and mortality rates, prolonged hospitalization periods, and substantial financial strain on healthcare systems. Meanwhile, the broad selection of naturally derived antibiotics, continuously augmented by novel semi-synthetic and fully synthetic antimicrobials [5, 6], has failed to resolve these issues, even as strategies for discovering and designing antibacterial compounds have evolved markedly [7, 8]. The management of MRSA-related infections is further hindered by the diverse mechanisms through which these bacteria acquire resistance determinants [1, 4, 6]. This concern intensified following the identification of vancomycin-resistant strains, given that vancomycin had long served as the primary therapeutic choice for MRSA cases [9].

A key approach in the pursuit of potent antistaphylococcal compounds involves studies focused on suppressing bacterial proliferation by interfering with signal transduction from DNA and RNA [10-15]. Critical enzymes involved in bacterial DNA replication and transcription include DNA gyrase, topoisomerase IIA, and topoisomerase IV, which represent prime targets for inhibitory agents [16, 17]. Numerous such inhibitors have been developed to date, yet efforts to launch novel DNA gyrase-targeting antimicrobials have largely faltered (as seen with Novobiocin) [10, 12], while the most recent candidate (Gepotidacin, GSK2140944) has progressed through clinical evaluation [18]. Thus, the intricate and multifaceted nature of resistance processes continues to drive the quest for innovative antibacterial therapies. Typically, these efforts emphasize structural optimizations of existing antibiotics and agents [15, 19-21], creation of novel low-molecular-weight compounds with targeted activity spectra [15, 22, 23], engineering of antimicrobial peptides [24], formation of transition metal-based antibacterial complexes [25], and similar directions. Among low-molecular-weight entities, hybrid molecules incorporating the 1,2,4-triazole scaffold stand out as particularly promising, offering opportunities for multi-target action mechanisms and demonstrating encouraging wide-ranging antibacterial effects against various significant clinical pathogens, including those resistant to conventional treatments [26-30]. Specifically, hybrids linking 1,2,4-triazole with azoles, coumarins, β-lactams, pyrimidines, quinolines, or quinazolines have exhibited strong potency against both susceptible and resistant microbes, often matching or surpassing standard frontline antibiotics. Furthermore, certain 1,2,4-triazole-3-thiones have demonstrated the capacity to reverse β-lactam resistance in laboratory strains of Escherichia coli and clinical isolates of Klebsiella pneumoniae by suppressing metallo-β-lactamase activity [31]. Accordingly, substituted 2-(3-R-1,2,4-triazol-5-yl)anilines emerge as compelling candidates for investigation; this selection is deliberate, primarily due to distinctive structural features [32, 33]. These compounds display conformational and configurational isomerism, generally possess modest molecular masses, and incorporate an optimal balance of hydrogen bond donors and acceptors through substitutions on the benzene ring and at the triazole's third position. They also allow modulation of key physicochemical properties, including solubility and lipophilicity. Additionally, their limited topological polar surface area suggests favorable penetration across the blood–brain barrier and adaptable binding to biological targets. Moreover, preliminary molecular docking simulations provided insights into binding interactions and comparable positioning within the active site of DNA gyrase (2XCT) for 2-(1,2,4-triazol-5-yl)aniline (TA) relative to the reference ligand, Ciprofloxacin **(Figure 1).**

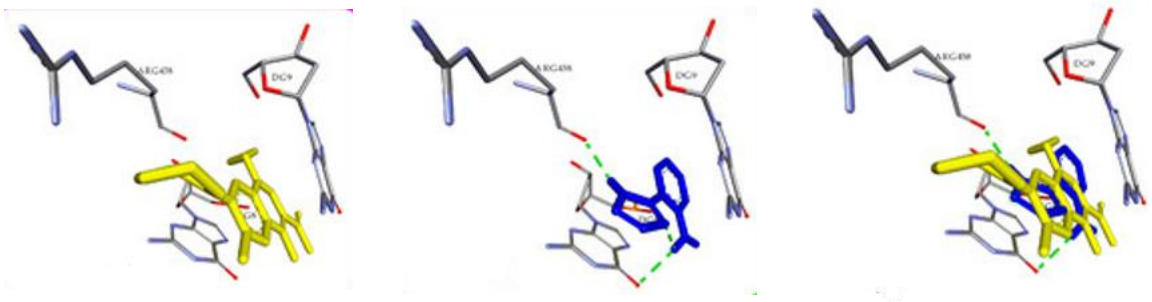

a) b) c)

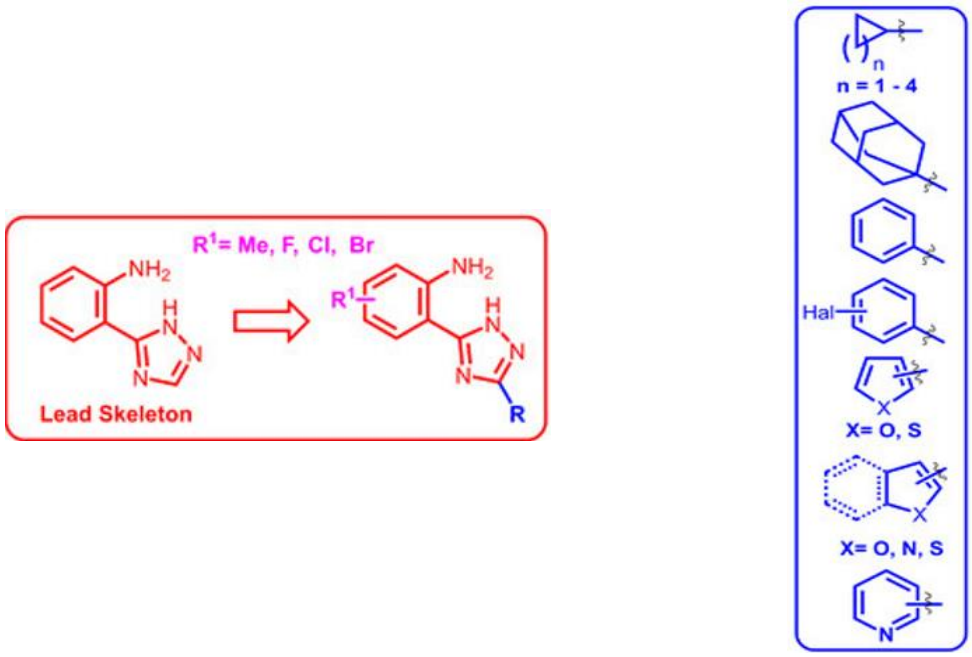

Figure 1. The proposed structures of the target compounds along with the binding conformations of the reference ligand, Ciprofloxacin (a), and 2-(1,2,4-triazol-5-yl)aniline (b), as well as their superimposed orientation (c) within the active site of DNA gyrase (2XCT).

Accordingly, the primary objectives of this investigation were to establish synthetic routes, assess the antistaphylococcal activity of previously underexplored hybrid compounds derived from the fusion of 2-(1,2,4-triazol-5-yl)aniline scaffolds with diverse pharmacophoric moieties **(Figure 1),** and perform molecular docking studies accompanied by qualitative and quantitative structure–activity relationship analyses to elucidate their prospects as potent antistaphylococcal therapeutics.

Materials and Methods

Synthetic procedures

Melting points were determined in open capillaries on a Mettler Toledo MP 50 instrument (Columbus, USA). Elemental composition (C, H, N) was analyzed using an ELEMENTAR vario EL cube instrument (Langenselbold, Germany), with deviations for analyzed elements or groups not exceeding ±0.3% from calculated values. ^{1}H and ^{13}C NMR spectra (at 500 MHz) were recorded on a Varian Mercury 500 instrument (Varian Inc., Palo Alto, CA, USA) in DMSO-d_6, with TMS as the internal reference. LC-MS analyses were performed on an Agilent 1100 Series HPLC system (Agilent, Palo Alto, CA, USA) coupled with a diode-array detector and an Agilent LC/MSD SL mass detector (Agilent, Palo Alto, USA) using atmospheric pressure chemical ionization (APCI).

General protocol for preparing [2-(3-R-1H-[1, 2, 4]triazol-5-yl)phenyl]amines (2.1–2.48).

Method A. To a suspension of 0.01 mol of the appropriate substituted 4-hydrazinoquinazoline (1.1–1.5) in 15 mL of glacial acetic acid, 0.82 g (0.01 mol) of sodium acetate was introduced, and the mixture was cooled to 0–5 °C. A solution of 0.01 mol of the selected commercial acyl chloride in 5 mL of glacial acetic acid (or a freshly prepared 0.01 mol acyl chloride solution in 15 mL of dioxane) was added dropwise while stirring. The mixture was maintained with continuous stirring for 30 min, followed by refluxing for 1.5–3 h, during which water (or the water–dioxane azeotrope) was continuously removed using a Dean–Stark apparatus. Upon reaction completion, the solvent was evaporated under reduced pressure. The residue was then treated with 10 mL of methanol, 10 mL of water, and 1 mL of concentrated hydrochloric acid, followed by 1 h of reflux. After cooling, the mixture was added to a saturated sodium acetate solution while adjusting the pH to 4–5. The precipitated product was collected by filtration, dried, and recrystallized from methanol or propan-2-ol.

Method B. A solution of 1.18 g (0.01 mol) of 2-aminobenzonitrile (3.1) in 5 mL of toluene was treated with 2.38 g (0.02 mol) of N,N-dimethylformamide dimethyl acetal (DMF-DMA) and 0.10 mL of acetic acid, then heated at 60 °C for 60 min. Excess DMF-DMA and toluene were removed completely under vacuum [34]. To the resulting residue, 0.01 mol of the appropriate carboxylic acid hydrazide and 10 mL of glacial acetic acid were added. The

mixture was refluxed for 1.5–3 h, with water removal via a Dean–Stark trap. Afterward, the solvent was evaporated to dryness under vacuum. The residue was then mixed with 10 mL of methanol, 10 mL of water, and 1 mL of concentrated hydrochloric acid, and refluxed for 1 h. Upon cooling, the mixture was poured into a saturated sodium acetate solution, maintaining pH at 4–5. The solid precipitate was filtered, dried, and recrystallized from methanol or propan-2-ol.

2-(3-Cyclopropyl-1H-1,2,4-triazol-5-yl)aniline (2.1): yield: 98.0% (Method A); mp 209–211 °C; 1H NMR, δ = 1.16–0.81 (m, 4H, cyclopropyl H-2,2,3,3), 2.13–1.97 (m, 1H, cyclopropyl H-1), 6.26 (br.s, 2H, NH2), 6.52 (t, J = 7.5 Hz, 1H, H-4), 6.69 (d, J = 8.1 Hz, 1H, H-6), 7.00 (t, J = 7.8 Hz, 1H, H-5), 7.76 (d, J = 6.9 Hz, 1H, H-3), 13.46 (br.s, 1H, NH); 13C NMR, δ 147.1 (aniline C-1), 130.1 (aniline C-3), 127.9 (aniline C-5), 116.2 (aniline C-4), 115.6 (aniline C-6), 101.7 (aniline C-2), 39.6 (cyclopropyl C-1), 8.2 (cyclopropyl C-2,3); LC-MS, m/z = 201 [M+1]; calculated for C11H12N4: C, 65.98; H, 6.04; N, 27.98; found: C, 65.96; H, 6.05; N, 27.97.

2-(3-Cyclopropyl-1H-1,2,4-triazol-5-yl)-6-methylaniline (2.2): yield: 90.1% (Method A); mp 158–160 °C; 1H NMR, δ = 0.92/1.05 (d, J = 6.7 Hz, 4H, cyclopropane H-2,2,3,3), 2.11–1.96 (m, 1H, cyclopropyl H-1), 2.15 (s, 3H, CH3), 6.30/5.93 (bs, 2H, NH2), 6.61–6.41 (m, 1H, H-4), 6.98/6.91 (d, J = 7.1 Hz, 1H, H-5), 7.79/7.51 (d, J = 7.9 Hz, 1H, H-3), 13.51/13.43 (br.s, 1H, NH); calculated for C12H14N4: C, 67.27; H, 6.59; N, 26.15; found: C, 67.26; H, 6.60; N, 26.15.

2-(3-Cyclopropyl-1H-1,2,4-triazol-5-yl)-5-fluoroaniline (2.3): yield: 97.7% (Method A); mp 242–244 °C; 1H NMR, δ = 1.04/0.91 (d, J = 6.7Hz, 4H, cyclopropyl H-2,2,3,3), 2.12–1.91 (m, 1H, cyclopropyl H-1), 6.33–6.16 (m, 1H, H-4), 6.53–6.33 (m, 3H, NH2, H-6), 6.86–6.77 (m, 1H, H-6), 7.87/7.63 (d, J = 7.8 Hz, 1H, H-3), 13.48/13.40 (br.s, 1H, NH); LC-MS, m/z = 219 [M+1]; calculated for C11H11FN4: C, 60.54; H, 5.08; N, 25.67; found: C, 60.51; H, 5.09; N, 25.66.

4-Chloro-2-(3-cyclopropyl-1H-1,2,4-triazol-5-yl)aniline (2.4): yield: 98.7% (Method A); mp 237–239 °C; 1H NMR, δ = 1.05/0.91 (d, J = 6.8 Hz, 4H, cyclopropyl H-2,2,3,3), 2.14–1.95 (m, 1H, cyclopropyl H-1), 6.28 (bs, 2H, NH2), 6.81–6.55 (m, 2H, H-6), 7.07–6.84 (m, 1H, H-5), 7.84/7.70 (s, 1H, H-3), 13.60/13.52 (br.s, 1H, NH); LC-MS, m/z = 235 [M+1]; calculated for C11H11ClN4: C, 56.30; H, 4.72; N, 23.87; found: C, 56.28; H, 4.74; N, 23.86.

2-(3-Cyclobutyl-1H-1,2,4-triazol-5-yl)aniline (2.5): yield: 77.1% (Method A); mp 147–149 °C; 1H NMR, δ = 2.18–1.88 (m, 2H, cyclobutyl H-3,3), 2.47–2.23 (m, 4H, H-2,2,4,4), 3.74–3.55 (m, 1H, cyclobutyl H-1), 6.27 (br. s, 2H, NH2), 6.54 (t, J = 7.5 Hz, 1H, H-4), 6.71 (d, J = 8.2 Hz, 1H, H-6), 7.13–6.94 (m, 1H, H-5), 7.92/7.66 (m, 1H, H-3), 13.58/13.45 (br.s, 1H, NH); LC-MS, m/z = 215 [M+1]; calculated for C12H14N4: C, 67.27; H, 6.59; N, 26.15; found: C, 67.26; H, 6.60; N, 26.15.

2-(3-Cyclobutyl-1H-1,2,4-triazol-5-yl)-6-methylaniline (2.6): yield: 92.2% (Method A); mp 127–129 °C; 1H NMR, δ = 2.12–1.90 (m, 2H, cyclobutyl H-3,3), 2.17 (s, 3H, CH3), 2.47–2.26 (m, 4H, cyclobutyl H-2,2,4,4), 3.82–3.49 (m, 1H, cyclobutyl H-1), 6.39/5.99 (bs, 2H, NH2), 6.52 (t, J = 7.6 Hz, 1H, H-4), 6.98/6.93 (m, 1H, H-5), 7.81/7.55 (m, 1H, H-3), 13.58/13.45 (bs, 1H, NH); LC-MS, m/z = 229 [M+1]; calculated for C13H16N4: C, 68.39; H, 7.06; N, 24.54; found: C, 68.38; H, 7.07; N, 24.55.

2-(3-Cyclobutyl-1H-1,2,4-triazol-5-yl)-5-fluoroaniline (2.7): yield: 94.8% (Method A); mp 165–167 °C; 1H NMR, δ = 2.17–1.86 (m, 2H, cyclobutyl H-3,3), 2.46–2.29 (m, 4H, cyclobutyl H-2,2,4,4), 3.76–3.47 (m, 1H, cyclobutyl H-1), 6.26 (d, J = 8.3 Hz, 1H, H-4), 6.61–6.33 (m, 3H, NH2, H-6), 7.07–6.79 (m, 1H, H-6), 7.93/7.65 (t, J = 8.0 Hz, 1H, H-3), 13.55/13.42 (bs, 1H, NH); LC-MS, m/z = 233 [M+1]; calculated for C12H13FN4: C, 62.06; H, 5.64; N, 24.12; found: C, 62.04; H, 5.65; N, 24.11.

4-Chloro-2-(3-cyclobutyl-1H-1,2,4-triazol-5-yl)aniline (2.8): yield: 99.3% (Method A); mp 176–178 °C; 1H NMR, δ = 2.21–1.86 (m, 2H, cyclobutyl H-3,3), 2.49–2.20 (m, 4H, cyclobutyl H-2,2,4,4), 3.78–3.52 (m, 1H, cyclobutyl H-1), 6.33 (bs, 2H, NH2), 6.72 (d, J = 8.6 Hz, 1H, H-6), 6.96 (d, J = 8.7 Hz, 1H, H-5), 7.90/7.73 (s, 1H, H-3), 13.65/13.53 (bs, 1H, NH); LC-MS, m/z = 249 [M+1]; calculated for C12H13ClN4: C, 57.95; H, 5.27; N, 22.53; found: C, 57.93; H, 5.29; N, 22.51.

2-(3-Cyclopentyl-1H-1,2,4-triazol-5-yl)aniline (2.9): yield: 65.7% (Method A); mp 100–102 °C; 1H NMR, δ = 2.19–1.55 (m, 8H, cyclopentyl H-2,2,3,3,4,4,5,5), 3 3.34–2.96 (m, 1H, cyclopentyl H-1), 6.18 (bs, 2H, NH2), 6.54 (t, J = 7.5 Hz, 1H, H-4), 6.79–6.65 (m, 1H, H-6), 7.15–6.85 (m, 1H, H-5), 7.92/7.63 (m, 1H, H-3), 13.55/13.42 (bs, 1H, NH); LC-MS, m/z = 229 [M+1]; calculated for C13H16N4: C, 68.39; H, 7.06; N, 24.54; found: C, 68.38; H, 7.08; N, 24.53.

2-(3-Cyclopentyl-1H-1,2,4-triazol-5-yl)-6-methylaniline (2.10): yield: 85.8% (Method A); mp 124–126 °C; 1H NMR, δ = 2.12–1.13 (m, 8H, cyclopentyl H-2,2,3,3,4,4,5,5), 2.16 (s, 3H, CH3) 3.34–3.10 (m, 1H, cyclopentyl H-

1), 6.37/5.97 (s, 2H, NH2), 6.55–6.45 (m, 1H, H-4), 6.98/6.92 (d, J = 6.8 Hz, 1H, H-5), 7.84/7.54 (d, J = 6.8 Hz, 1H, H-3), 13.52/13.40 (s, 1H, NH); LC-MS, m/z = 243 [M+1]; calculated for C14H18N4: C, 69.39; H, 7.49; N, 23.12; found: C, 69.38; H, 7.50; N, 23.13.

2-(3-Cyclopentyl-1H-1,2,4-triazol-5-yl)-5-fluoroaniline (2.11): yield: 80.8% (Method A); mp 112–114 °C; 1H NMR, δ = 2.18–1.54 (m, 8H, cyclopentyl H-2,2,3,3,4,4,5,5), 3.20 (p, J = 8.2 Hz, 1H, cyclopentyl H-1), 6.26 (t, J = 8.5 Hz, 1H, H-4), 6.46 (d, J = 8.5 Hz, 1H, H-6), 6.72 (bs, 2H, NH2), 8.02–7.65 (m, 1H, H-3), 13.39 (bs, 1H, NH); LC-MS, m/z = 247 [M+1]; calculated for C13H15FN4: C, 63.40; H, 6.14; N, 22.75; found: C, 63.38; H, 6.15; N, 22.76.

4-Chloro-2-(3-cyclopentyl-1H-1,2,4-triazol-5-yl)aniline (2.12): yield: 96.3% (Method A); mp 161–163 °C; 1H NMR, δ = 2.19–1.51 (m, 8H, cyclopentyl H-2,2,3,3,4,4,5,5), 3.21 (p, J = 8.4 Hz, 1H, cyclopentyl H-1), 6.33 (bs, 2H, NH2), 6.72 (d, J = 8.8 Hz, 1H, H-6), 6.96 (d, J = 8.6 Hz, 1H, H-5), 7.88 (s, 1H, H-3), 13.51 (bs, 1H, NH); LC-MS, m/z = 263 [M+1]; calculated for C13H15ClN4: C, 59.43; H, 5.75; N, 21.32; found: C, 59.42; H, 5.76; N, 21.31.

2-(3-Cyclohexyl-1H-1,2,4-triazol-5-yl)aniline (2.13): yield: 89.3% (Method A); mp 152–154 °C; 1H NMR, δ = 1.78–1.22 (m, 6H, cyclohexyl H-3eq, 4eq, 5eq, 3ax, 4ax, 5ax), 1.91–1.78 (m, 2H, cyclohexyl H-2ax, 6ax), 2.10–1.95 (m, 2H, cyclohexyl H-2eq, 6eq), 2.90–2.63 (m, 1H, cyclohexyl H-1), 6.17 (bs, 1H, NH2), 6.63–6.42 (m, 2H, H-4, NH2), 6.81–6.63 (m, 1H, H-6), 7.12–6.90 (m, 1H, H-5), 7.91/7.62 (d, J = 7.9 Hz, 1H, H-3), 13.53/13.37 (bs, 1H, NH); 13C NMR, δ = 147.1 (aniline C-1), 130.0 (aniline C-3), 127.9 (aniline C-5), 116.2 (aniline C-4), 115.6 (aniline C-6), 98.3 (aniline C-2), 36.2 (cyclohexane C-1), 31.6 (cyclohexane C-2,6), 25.9 (cyclohexane C-3,5), 25.8 (cyclohexane C-4); calculated for C14H18N4: C, 69.39; H, 7.49; N, 23.12; found: C, 69.37; H, 7.51; N, 23.13.

2-(3-Cyclohexyl-1H-1,2,4-triazol-5-yl)-6-methylaniline (2.14): yield: 91.3% (Method A); mp 135–137 °C; 1H NMR, δ = 1.79–1.16 (m, 6H, cyclohexyl H-3eq, 4eq, 5eq, 3ax, 4ax, 5ax), 1.92–1.79 (m, 2H, cyclohexyl H-2ax, 6ax), 2.10–1.95 (m, 2H, cyclohexyl H-2eq, 6eq), 2.17 (s, 3H, CH3), 2.85–2.73 (m, 1H, cyclohexyl H-1), 6.20 (bs, 2H, NH2), 6.51 (t, J = 7.5 Hz, 1H, H-4), 6.95 (d, J = 7.2 Hz, 1H, H-5), 7.93–7.55 (m, 1H, H-3), 13.50 (bs, 1H, NH); LC-MS, m/z = 257 [M+1]; calculated for C15H20N4: C, 70.28; H, 7.86; N, 21.86; found: C, 70.26; H, 7.88; N, 21.85.

2-(3-Cyclohexyl-1H-1,2,4-triazol-5-yl)-5-fluoroaniline (2.15): yield: 89.0% (Method A); mp 151–153 °C; 1H NMR, δ = 1.77–1.20 (m, 6H, cyclohexyl H-3eq, 4eq, 5eq, 3ax, 4ax, 5ax), 1.93–1.78 (m, 2H, cyclohexyl H-2ax, 6ax), 2.14–1.93 (m, 2H, cyclohexyl H-2eq, 6eq), 2.89–2.62 (m, 1H, cyclohexyl H-1), 6.33–6.13 (m, 1H, H-4), 6.66–6.33 (m, 2H, NH2, H-6), 6.91 (bs, 1H, NH), 7.91/7.65 (d, J = 10.3 Hz, 1H, H-3), 13.50/13.36 (s, 1H, NH); LC-MS, m/z = 261 [M+1]; calculated for C14H17FN4: C, 64.60; H, 6.58; N, 21.52; found: C, 64.59; H, 6.59; N, 21.51.

4-Chloro-2-(3-cyclohexyl-1H-1,2,4-triazol-5-yl)aniline (2.16): yield: 93.9% (Method A); mp 200–202 °C; 1H NMR, δ = 1.77–1.16 (m, 6H, cyclohexyl H-3eq, 4eq, 5eq, 3ax, 4ax, 5ax), 1.92–1.78 (m, 2H, cyclohexyl H-2ax, 6ax), 2.15–1.92 (m, 2H, cyclohexyl H-2eq, 6eq), 2.90–2.62 (m, 1H, cyclohexyl H-1), 6.33 (bs, 2H, NH2), 6.71 (d, J = 8.6 Hz, 1H, H-6), 6.95 (d, J = 8.6 Hz, 1H, H-5), 7.88/7.73 (s, 1H, H-3), 13.62/13.47 (bs, 1H, NH); LC-MS, m/z = 277 [M+1]; calculated for C14H17ClN4: C, 60.76; H, 6.19; N, 20.24; found: C, 60.75; H, 6.21; N, 20.23.

2-(3-(Adamantan-1-yl)-1H-1,2,4-triazol-5-yl)aniline (2.17): yield: 94.1% (Method A), 73.4% (Method B); mp 150–152 °C; 1H NMR, δ = 1.81–1.71 (m, 6H, adamantyl-4,4,6,6,10,10), 2.09–1.98 (m, 9H, adamantyl-2,2,3,5, 7,8,8,9,9), 5.49 (bs, 2H, NH2), 6.90 (t, J = 7.4 Hz, 1H, H-4), 7.04 (d, J = 7.8 Hz, 1H, H-6), 7.24 (d, J = 7.2 Hz, 1H, H-5), 7.97 (d, J = 7.4 Hz, 1H, H-3); 13C NMR, δ = 171.5 (triazole C-5), 158.1 (triazole C-3), 141.4 (aniline C-1), 132.1 (aniline C-3), 131.4 (aniline C-5), 120.2 (aniline C-4), 119.3 (aniline C-6), 40.9 (adamantane C-2, 8, 9), 38.9 (adamantane C-6), 36.4 (adamantane C-4, 6, 10), 28.0 (adamantane C-3, 5, 7); LC-MS, m/z = 295 [M+1]; calculated for C18H22N4: C, 73.44; H, 7.53; N, 19.03; found: C, 73.42; H, 7.55; N, 19.05.

2-(3-(Adamantan-1-yl)-1H-1,2,4-triazol-5-yl)-6-methylaniline (2.18): yield: 96.3% (Method A); mp 197–199 °C; 1H NMR, δ = 1.91–1.70 (m, 6H, adamantyl-4,4,6,6,10,10), 2.14–1.94 (m, 9H, adamantyl-2,2,3,5, 7,8,8,9,9), 2.17 (s, 3H, adamantyl-CH3), 6.20 (bs, 2H, NH2), 6.52 (t, J = 7.5 Hz, 1H, H-4), 6.95 (d, J = 7.2 Hz, 1H, H-5), 7.75 (d, J = 7.5 Hz, 1H, H-3), 13.45 (br.s, 1H, NH); LC-MS, m/z = 309 [M+1]; calculated for C19H24N4: C, 73.99; H, 7.84; N, 18.17; found: C, 73.98; H, 7.85; N, 18.17.

2-(3-(Adamantan-1-yl)-1H-1,2,4-triazol-5-yl)-5-fluoroaniline (2.19): yield: 97.9% (Method A); mp 274–276 °C; 1H NMR, δ = 1.92–1.68 (m, 6H, adamantyl-4,4,6,6,10,10), 2.21–1.92 (m, 9H, adamantyl-2,2,3,5, 7,8,8,9,9), 6.23

(d, J = 8.7 Hz, 1H, H-4), 6.94–6.33 (m, 3H, NH2, H-6), 8.02–7.73 (m, 1H, H-3), 13.33 (s, 1H, NH); LC-MS, m/z = 313 [M+1]; calculated for C18H21FN4: C, 69.21; H, 6.78; N, 17.94; found: C, 69.20; H, 6.79; N, 17.94.

2-(3-(Adamantan-1-yl)-1H-1,2,4-triazol-5-yl)-4-chloroaniline (2.20): yield: 96.4% (Method A); mp 243–245 °C; 1H NMR, δ = 1.90–1.66 (m, 6H, adamantyl-4,4,6,6,10,10), 2.20–1.91 (m, 9H, adamantyl-2,2,3,5, 7,8,8,9,9), 6.32 (bs, 2H, NH2), 6.71 (d, J = 8.9 Hz, 1H, H-6), 6.95 (d, J = 8.6 Hz, 1H, H-5), 7.90/7.73 (s, 1H, H-3), 13.61/13.46 (s, 1H, NH); LC-MS, m/z = 329 [M+1]; calculated for C18H21ClN4: C, 65.74; H, 6.44; N, 17.04; found: C, 65.73; H, 6.44; N, 17.03.

2-(3-(Adamantan-1-yl)-1H-1,2,4-triazol-5-yl)-4-bromoaniline (2.21): yield: 88.9% (Method A); mp 249–251 °C; 1H NMR, δ = 1.89–1.69 (m, 6H, adamantyl-4,4,6,6,10,10), 2.22–1.92 (m, 9H, adamantyl-2,2,3,5, 7,8,8,9,9), 6.36 (br.s, 2H, NH2), 6.68 (d, J = 8.7 Hz, 1H, H-6), 7.07 (d, J = 8.6 Hz, 1H, H-5), 8.01 (s, 1H, H-3), 13.45 (bs, 1H, NH); LC-MS, m/z = 373 [M+1]; calculated for C18H21BrN4: C, 57.92; H, 5.67; N, 15.01; found: C, 57.90; H, 5.69; N, 15.03.

2-(3-Phenyl-1H-1,2,4-triazol-5-yl)aniline (2.22): yield: 96.9% (Method A), 94.9% (Method B); mp 189–191 °C; 1H NMR, δ = 6.63 (t, J = 7.4 Hz, 1H, H-4), 6.72 (br s, 2H, NH2), 6.83 (d, J = 7.7 Hz, 1H, H-6), 7.14 (t, J = 7.5, 1H, H-5), 7.49 (m, 3H, 3-Ar H-3,4,5), 7.78 (d, J = 7.7 Hz, 1H, H-3), 8.09 (d, J = 7.0 Hz, 2H, 3-Ar H-2,6), 14.48/14.20 (br.s, 1H, NH); 13C NMR, δ = 160.7 (triazole C-3), 154.1 (triazole C-5), 147.4 (aniline C-1), 131.4 (phenyl C-1, 3, 4, 5), 129.2 (aniline C-5), 127.4 (phenyl C-2,6), 126.4 (aniline C-3), 116.5 (aniline C-4), 115.2 (aniline C-6), 108.9 (aniline C-2); LC-MS, m/z = 237 [M+1]; calculated for C14H12N4: C, 71.17; H, 5.12; N, 23.71; found: C, 71.23; H, 5.19; N, 23.75.

2-(3-(4-Fluorophenyl)-1H-1,2,4-triazol-5-yl)aniline (2.23): yield: 93.6% (Method A), 90.6% (Method B); mp 209–211 °C; 1H NMR, δ = 6.64 (t, J = 7.0 Hz, 1H, H-4), 6.85 (d, J = 7.8 Hz, 1H, H-6), 7.15 (t, J = 7.3 Hz, 1H, H-5), 7.34 (t, J = 7.7 Hz, 2H, 3-Ar H-3,5), 7.92–7.75 (d, J = 7.3 Hz, 1H, H-3), 8.13 (t, J = 6.7 Hz, 2H, 3-Ar H-2,6), 14.36 (bs, 1H, NH); 13C NMR, δ = 162.7 (d, J = 253.4 Hz, phenyl C-4), 159.4 (triazole C-3), 155.6 (triazole C-5), 146.7 (aniline C-1), 130.5 (phenyl C-1), 130.0 (aniline C-5), 128.0 (d, J = 7.7 Hz, phenyl C-2,6), 127.2 (aniline C-3), 116.1 (aniline C-4), 115.7 (d, J = 22.3 Hz, phenyl C-3,5), 115.2 (aniline C-6), 108.0 (aniline C-2); LC-MS, m/z = 255 [M+1]; calculated for C14H11FN4: C, 66.13; H, 4.36; N, 22.03; found: C, 66.17; H, 4.41; N, 22.27.

2-(3-(4-Chlorophenyl)-1H-1,2,4-triazol-5-yl)aniline (2.24): yield: 92.6% (Method A), 93.2% (Method B); mp 289–291 °C; 1H NMR, δ = 6.99–6.51 (m, 3H, H-4, NH2), 7.16 (m, 1H. H-6), 7.57 (d, J = 6.3 Hz, 1H, H-5), 7.98–7.77 (m, 2H, 3-Ar H-3,5), 8.11 (d, J = 7.0 Hz, 1H, H-3), 8.30 (d, J = 7.1 Hz, 2H, 3-Ar H-2,6; 13C NMR, δ = 161.9 (triazole C-3), 157.5 (triazole C-5), 146.9 (aniline C-1), 134.1 (phenyl C-4), 130.5 (aniline C-5), 128.8 (phenyl C-3,5), 126.4 (phenyl C-2,6), 125.7 (aniline C-3), 116.0 (aniline C-4), 115.1 (aniline C-6), 108.7 (aniline C-2); LC-MS, m/z = 271 [M+1]; calculated for C14H11ClN4: C, 62.11; H, 4.10; N, 20.70; found: C, 62.19; H, 4.16; N, 20.77.

2-(3-(4-Bromophenyl)-1H-1,2,4-triazol-5-yl)aniline (2.25): yield: 95.5% (Method A), 96.2% (Method B); mp 216–218 °C; 1H NMR, δ = 6.63 (t, J = 7.3 Hz, 1H, H-4); 6.85 (d, J = 8.0 Hz, 1H, H-6), 7.15 (t, J = 7.3 Hz, 1H, H-5), 7.62 (d, J = 8.0 Hz, 1H, H-3), 7.66 (d, J = 7.9 Hz, 2H, 3-Ar H-3,5), 7.85 (d, J = 8.0 Hz, 2H, 3-Ar H-2,6); 13C NMR, δ = 162.6 (triazol C-3), 158.8 (triazol C-5), 146.7 (aniline C-1), 131.5 (phenyl C-3,5), 131.1 (phenyl C-2,6), 130.9 (aniline C-5), 129.8 (phenyl C-1), 124.8 (aniline C-3), 122.0 (phenyl C-4), 116.1 (aniline C-4), 115.2 (aniline C-6), 110.9 (aniline C-2); LC-MS, m/z = 316 [M+1]; calculated for C14H11BrN4: C, 53.35; H, 3.52; N, 17.78; found: C, 53.41; H, 3.57; N, 17.82.

2-(3-(2-Fluorohenyl)-1H-1,2,4-triazol-5-yl)aniline (2.26): yield: 91.3% (Method A), 89.6% (Method B); mp 195–197 °C; 1H NMR, δ = 6.65 (t, J = 7.3 Hz, 1H, H-4), 6.75 (bs, 2H, NH2), 6.85 (d, J = 8.1 Hz, 1H, H-6), 7.15 (t, J = 7.2 Hz, 1H, H-5), 7.41–7,30 (m, 2H, 3-Ar H-3, 5), 7.55–7.46 (m, 1H, 3-Ar H-4), 7.93–7.81 (m, 1H, H-3), 8.11 (t, J = 7.3 Hz, 1H, 3-Ar H-6), 14.36 (bs, 1H, NH); 13C NMR, δ = 162.8 (triazol C-3), 159.3 (d, J = 253.2 Hz, phenyl C-2), 154.7 (triazol C-5), 146.8 (aniline C-1), 131.1 (aniline C-5), 130.3 (phenyl C-4), 129.7 (d, J = 2.6 Hz, phenyl C-5), 127.2 (phenyl C-6), 124.6 (aniline C-3), 116.4 (d, J = 21.2 Hz, phenyl C3), 116.0 (aniline C-4), 115.2 (aniline C-6), 109.3 (aniline C-2); LC-MS, m/z = 255 [M+1]; calculated for C14H11FN4: C, 66.13; H, 4.36; N, 22.03; found: C, 66.19; H, 4.39; N, 22.17.

2-(3-(Furan-2-yl)-1H-1,2,4-triazol-5-yl)aniline (2.27): yield: 86.3% (Method A), 73.10% (Method B); mp 206–208 °C; 1H NMR, δ = 6.71–6.61 (m, 2H, H-4, furan, H-4), 6.85 (d, 1H, J = 8.2 Hz, H-6), 7.10–6.99 (m, 1H, furan, H-3), 7.17 (t, 1H, J = 8.2 Hz, H-5), 7.94–7.80 (m, 2H, H-6, furan H-3); calculated for C12H10N4O: C, 63.71; H, 4.46; N, 24.76; found: C, 63.70; H, 4.47; N, 24.75.

2-(3-(Furan-3-yl)-1H-1,2,4-triazol-5-yl)-6-methylaniline (2.28): yield: 72.25% (Method B); mp 182–184 °C; 1H NMR, δ = 2.19 (s, 3H, CH3), 6.42/6.02 (br. s, 2H, NH2), 6.55 (t, J = 7.2 Hz, 1H, H-4), 7.09–6.81 (m, 2H, H-5, furan, H-4), 7.73–7.50 (m, 2H, H-3, furan, H-5), 7.91 (d, J = 7.9 Hz, 1H, H-3), 8.25/8,03 (bs, 1H, furan, H-2), 14.07/13.93 (s, 1H, NH); LC-MS, m/z = 241 [M+1]; calculated for C13H12N4O: C, 64.99; H, 5.03; N, 23.32; found: C, 64.97; H, 23.33.

5-Fluoro-2-(3-(furan-3-yl)-1H-1,2,4-triazol-5-yl)aniline (2.29): yield: 79.98% (Method A); mp 204–206 °C; 1H NMR, δ = 6.66–6.15 (m, 3H, H-4, NH2), 7.11–6.79 (m, 2H, H-6, furan H-4), 7.64/7.57 (m, 1H, H-5), 7.99/7.72 (t, J = 7.8 Hz, 1H, H-3), 8.21/8.08 (s, 1H, furan, H-2), 14.04/13.90 (s, 1H, NH); LC-MS, m/z = 245 [M+1]; calculated for C12H9FN4O: C, 59.02; H, 3.71; N, 22.94; found: C, 59.00; H, 3.71; N, 22.95.

4-Chloro-2-(3-(furan-3-yl)-1H-1,2,4-triazol-5-yl)aniline (2.30): yield: 77.99% (Method A); mp 248–250 °C; 1H NMR, δ = 6.38 (s, 2H, NH2), 6.85–6.70 (m, 1H, H-6), 7.10–6.86 (m, 2H, H-5, furan, H-4), 7.66/7.58 (m, 1H, furan, H-5), 7.96/7.79 (s, 1H, H-3), 8.24/8.08 (m, 1H, furan H-2), 14.15/14.01 (s, 1H, NH); LC-MS, m/z = 261 [M+1]; anal. calcd. for C12H9ClN4O: C, 55.29; H, 3.48; N, 21.49; found: C, 55.27; H, 3.49; N, 21.50.

4-Bromo-2-(3-(furan-3-yl)-1H-1,2,4-triazol-5-yl)aniline (2.31): yield: 56.00% (Method A); mp 228–230 °C; 1H NMR, δ = 6.51 (s, 2H, NH2), 6.73 (d, J = 8.8 Hz, 1H, H-6), 7.06–6.84 (m, 1H, H-5), 7.12 (d, J = 8.2 Hz, 1H, furan H-4), 7.63 (d, J = 7.8 Hz, 1H, furan, H-5), 8.37–7.86 (m, 2H, H-3, furan H-2), 14.18 (s, 1H, NH); calculated for C12H9BrN4O: C, 47.24; H, 2.97; N, 18.36; found: C, 47.21; H, 2.98; N, 18.37.

2-(3-(Thiophen-2-yl)-1H-1,2,4-triazol-5-yl)aniline (2.32): yield: 98.63% (Method A), 92.3% (Method B); mp 189–191 °C; 1H NMR, δ = 6.65 (t, 1H, J = 8.3 Hz, H-4), 6.85 (d, 1H, J = 8.3 Hz, H-6), 7.19 (m, 2H, H-4, thiophen, H-5), 7.66 (d, 1H, thiophen, H-3), 7.72 (d, 1H, thiophen, H-5), 7,81 (d, 1H, H-3); 13C NMR, δ = 147.6 (aniline C-1), 134.4 (thiophen C-2), 131.5 (aniline C-3), 128.4 (aniline C-5), 127.4 (thiophen C-5), 127.3 (thiophen C-4), 126.3 (thiophen C-3), 116.8 (aniline C-4), 115.7 (aniline C-6), 107.9 (aniline C-2); LC-MS, m/z = 243 [M+1]; calculated for C12H10N4S: C, 59.48; H, 4.16; N, 23.12; found: C, 59.46; H, 4.18; N, 20.85.

5-Fluoro-2-(3-(thiophen-2-yl)-1H-1,2,4-triazol-5-yl)aniline (2.33): yield: 96.76% (Method A); mp 233–235 °C; 1H NMR, δ = 6.31 (bs, 2H, NH2), 6.69–6.42 (m, 1H, H-4), 7.01–6.81 (m, 1H, H-6), 7.19–7.05 (m, 1H, thiophene, H-4), 7.47–7.27 (m, 1H, thiophene, H-3), 7.63/7.56 (m, 1H, thiophene, H-5), 8.01/7.73 (m, 1H, H-3), 14.26/13.99 (s, 1H, NH); LC-MS, m/z = 261 [M+1]; calculated for C12H9FN4S: C, 55.37; H, 3.49; N, 21.53; found: C, 55.35; H, 3.49; N, 21.50.

6-Methyl-2-(3-(thiophen-3-yl)-1H-1,2,4-triazol-5-yl)aniline (2.34): yield: 98.75% (Method A); mp 168–170 °C; 1H NMR, δ = 2.20 (s, 3H, CH3), 6.35 (s, 2H, NH2), 6.56 (t, J = 7.4 Hz, 1H, H-4), 7.00 (d, J = 5.6 Hz, 1H, thiophene H-4), 7.59–7.42 (m, 1H, H-5), 7.78 -7.60 (m, 2H, H-2, 5 thiophene), 8.09–7.80 (bs, 3H, H-3), 13.97 (s, 1H, NH); LC-MS, m/z = 257 [M+1]; calculated for C13H12N4S: C, 60.92; H, 4.72; N, 21.86; found: C, 60.91; H, 4.74; N, 21.86.

5-Fluoro-2-(3-(thiophen-3-yl)-1H-1,2,4-triazol-5-yl)aniline (2.35): yield: 80.18% (Method A); mp 212–214 °C; 1H NMR, δ = 6.30 (bs, 1H, NH2), 6.69–6.41 (m, 2H, H-4, NH), 7.11–6.92 (m, 1H, H-6), 7.66–7.33 (m, 2H, H-4.5 thiophene), 8.01/7.71 (m, 1H, H-3), 8.11/7.93 (m, 1H, H-2 thiophene), 14.12/13.91 (s, 1H, NH); LC-MS, m/z = 261 [M+1]; calculated for C12H9FN4S: C, 55.37; H, 3.49; N, 21.53; found: C, 55.35; H, 3.52; N, 21.54.

4-Chloro-2-(3-(thiophen-3-yl)-1H-1,2,4-triazol-5-yl)aniline (2.36): yield: 75.28% (Method A); mp 240–242 °C; 1H NMR, δ = 6.41 (bs, 2H, NH2), 6.90–6.66 (m, 1H, H-6), 7.10–6.92 (m, 1H, H-5), 7.55/7.46 (m, 1H, H-4 thiophene), 7.71/7.64 (m, 1H, H-5 thiophene), 7.97 (s, 1H, H-3), 8.14 (s, 1H, H-2 thiophene), 14.24/14.03 (s, 1H, NH); LC-MS, m/z = 277 [M+1]; calculated for C12H9ClN4S: C, 52.08; H, 3.28; N, 20.25; found: C, 52.06; H, 3.30; N, 20.26.

4-Bromo-2-(3-(thiophen-3-yl)-1H-1,2,4-triazol-5-yl)aniline (2.37): yield: 77.13% (Method A); mp 235–236 °C; 1H NMR, δ = 6.44 (s, 2H, NH2), 6.97–6.60 (m, 1H, H-6), 7.24–7.02 (m, 1H, H-5), 7.55/7.46 (m, 1H, H-4 thiophene), 7.71/7.63 (m, 1H, H-5 thiophene), 7.94 (s, 1H, H-3), 8.12 (s, 1H, H-2 thiophene), 14.23/14.02 (s, 1H, NH); LC-MS, m/z = 322 [M+1]; calculated for C12H9BrN4S: C, 44.87; H, 2.82; N, 17.44; found: C, 44.86; H, 2.85; N, 17.45.

2-(3-(Benzofuran-2-yl)-1H-1,2,4-triazol-5-yl)aniline (2.38): yield: 65.21% (Method A), 71.3% (Method B); mp 235–237 °C; 1H NMR, δ = 5.45 (bs, 2H, NH2), 6.71 (t, 1H, J = 8.3 Hz, H-4), 6.90 (d, 1H, J = 8.3 Hz, H-6), 7.45–7.12 (m, 3H, H-5, benzofuran, H-5, H-6), 7.56 (s, 1H, benzofuran, H-3), 7.76–7.64 (m, benzofuran, H-4,7), 7.91 (d, J = 7.1 Hz, 1H, H-3); 13C NMR, δ = 158.4 (triazole C-5), 154.9 (benzofuran C-7a), 154.7 (triazole C-3), 148.9 (benzofuran C-2), 147.6 (aniline C-1), 131.5 (aniline C-3), 128.4 (aniline C-5), 127.8 (benzofuran C-3a), 124.1 (benzofuran C-6), 123.1 (benzofuran C-5), 122.2 (benzofuran C-4), 116.7 (aniline C-4), 115.8 (aniline C-6), 111.9

(benzofuran C-7), 109.2 (benzofuran C-3), 106.0 (aniline C-2); LC-MS, m/z = 277 [M+1]; calculated for C16H12N4O: C, 69.55; H, 4.38; N, 20.28; found: C, 69.55; H, 4.40; N, 20.29.

2-(3-(Benzofuran-2-yl)-1H-1,2,4-triazol-5-yl)-6-methylaniline (2.39): yield: 92.50% (Method A); mp 200–201 °C; 1H NMR, δ = 2.21 (s, 3H, CH3), 6.57 (m, 3H, H-4, NH2), 7.05 (d, J = 7.2 Hz, 1H, H-5), 7.48–7.16 (m, 3H, H-3, 5, 6 benzofuran), 7.84–7.48 (m, 3H, H-3, benzofuran, H-4,7), 14.72/14.31 (s, 1H, NH); LC-MS, m/z = 291 [M+1]; anal. calcd. for C17H14N4O: C, 70.33; H, 4.86; N, 19.30; found: C, 70.30; H, 4.88; N, 19.31.

2-(3-(Benzofuran-2-yl)-1H-1,2,4-triazol-5-yl)-5-fluoroaniline (2.40): yield: 50.78% (Method A); mp 251–253 °C; 1H NMR, δ = 6.32 (s, 2H, NH2), 6.55 (t, J = 8.0 Hz, 1H, H-4), 7.09–6.99 (m, 1H, H-6), 7.44–7.12 (m, 3H, H-3,5,6 benzofuran), 8.07–7.88 (m, 2H, H-4,7 benzofuran), 8.17 (dt, J = 8.9, Hz, 1H, H-3), 12.21 (s, 1H, NH); LC-MS, m/z = 295 [M+1]; calculated for C16H11FN4O: C, 65.30; H, 3.77; N, 19.04; found: C, 65.29; H, 3.79; N, 19.05.

2-(3-(Benzofuran-2-yl)-1H-1,2,4-triazol-5-yl)-4-chloroaniline (2.41): yield: 75.72% (Method A); mp 245–246 °C; 1H NMR, δ = 6.43 (bs, 2H, NH2), 6.88–6.74 (m 1H, H-6), 7.13–6.93 (m, 1H, H-5), 7.46–7.18 (m, 3H, H-3,5,6 benzofuran), 7.72–7.50 (m, 2H, H-4,7 benzofuran), 7.84 (s, 1H, H-3), 14.81/14.42 (s, 1H, NH); LC-MS, m/z = 311 [M+1]; anal. calcd. for C16H11ClN4O: C, 61.84; H, 3.57; N, 18.03; found: C, 61.84; H, 3.59; N, 18.04.

2-(3-(Benzofuran-2-yl)-1H-1,2,4-triazol-5-yl)-4-bromoaniline (2.42): yield: 90.58% (Method A); mp 224–226 °C; 1H NMR, δ = 6.47 (bs, 2H, NH2), 6.84–6.66 (d, 1H, H-6), 6.97–6.81 (m, 1H, H-5), 7.20–7.04 (m, 1H, H-5 benzofuran), 7.29–7.22 (t, 1H, H-6 benzofuran), 7.38–7.28 (m, 1H, H-3 benzofuran), 7.87–7.50 (m, 2H, H-4,7 benzofuran), 7.98 (s, 1H, H-3), 14.80/14.39 (s, 1H, NH); LC-MS, m/z = 356 [M+1]; calculated for C16H11BrN4O: C, 54.10; H, 3.12; N, 15.77; found: C, 54.08; H, 3.14; N, 15.78.

2-(3-(Benzo[b]thiophen-2-yl)-1H-1,2,4-triazol-5-yl)aniline (2.43): yield: 98.6% (Method A); mp 192–196 °C; 1H NMR, δ = 6.70 (t, 1H, J = 8.3 Hz, H-5), 6.90 (d, 1H, J = 8.3 Hz, H-3), 7.21 (t, 1H, J = 8.3 Hz, H-4), 7.44 (m, 2H, H-5 H6 benzo[b]thiophen), 7.83 (d, 1H, J = 8,3 Hz, H-6), 7.97 (d, J = 5.0 Hz, 1H, H-4 benzo[b]thiophen), 8,03 (d, J = 5.0 Hz, 1H, H-7 benzo[b]thiophen), 8,08 (s, 1H, H-3 benzo[b]thiophen); LC-MS, m/z = 293 [M+1]; calculated for C16H12N4S: C, 65.73; H, 4.14; N, 19.16; found: C, 65.78; H, 4.19; N, 19.22.

2-(3-(1H-Indol-2-yl)-1H-1,2,4-triazol-5-yl)aniline (2.44): yield: 61.70% (Method A); mp 242–244 °C; 1H NMR, δ = 6.70 (t, J = 8.1 Hz, 1H, H-5), 6.91 (d, J = 8.1 Hz, 1H, H-3), 7.07 (m, 2H, indol, H-5, H-6), 7.23 (m, 2H, indol, H-3, H-4), 7.48 (d, 1H, indol, H-4), 7.62 (d, 1H, indol, H-7), 7.89 (d, 1H, J = 7.8 Hz, H-6), 11.86 (s, 1H, NH), 12.14 (s, 1H, NH); LC-MS, m/z = 276 [M+1]; calculated for C16H13N5: C, 69.80; H, 4.76; N, 25.44; found: C, 69.78; H, 4.77; N, 25.45.

2-(3-(Pyridin-2-yl)-1H-1,2,4-triazol-5-yl)aniline (2.45): yield: 86.21% (Method A); mp 185–186 °C; 1H NMR, δ = 6.28 (s, 2H, NH2), 6.59 (t, J = 7.5 Hz, 1H, H-4), 6.75 (m, 1H, H-6), 7.05 (t, J = 7.8 Hz, H-5), 7.46/7.35 (m, 1H, H-3), 7.95 (t, J = 7.7 Hz, 1H, pyridine, H-5), 8.04 (d, J = 7.8 Hz, 1H, pyridine, H-3), 8.23 (d, J = 7.8 Hz, 1H, pyridine, H-6), 8.69 (m, 1H, pyridine, H-4), 14.58/14.23 (s, 1H, NH); 13C NMR, δ = 162.8 (triazole C-5), 153.7 (triazole C-3), 150.1 (pyridine C-6), 147.1 (aniline C-1), 146.6 (pyridine C-2), 138.4 (pyridine C-4), 131.5 (aniline C-3), 128.5 (aniline C-5), 125.7 (pyridine C-5), 122.0 (pyridine C-3), 116.7 (aniline C-4), 115.8 (aniline C-6), 112.9 (aniline C-2); LC-MS, m/z = 238 [M+1]; calculated for C13H11N5: C, 65.81; H, 4.67; N, 29.52; found: C, 65.82; H, 4.68; N, 29.54.

2-(3-(Pyridin-3-yl)-1H-1,2,4-triazol-5-yl)aniline (2.46): yield: 81.3% (Method A), 90.3% (Method B); mp 245–246 °C; 1H NMR, δ = 6.59 (t, J = 7.4 Hz, 1H, H-4), 6.67 (s, 1H, NH2), 6.81 (d, J = 8.2 Hz, 1H, H-6), 7.11 (t, J = 7.6 Hz, 1H, H-5), 7.41 (t, J = 6.3, Hz, 1H, pyridine, H-5), 7.72 (d, J = 7.5 Hz, 1H, H-3), 8.39 (d, J = 8.2 Hz, 1H, pyridine, H-4), 8.57 (d, J = 8.4 Hz, 1H, pyridine, H-6), 9.26 (s, 1H, pyridine, H-2), 14.51/14.20 (s, 1H, NH); 13C NMR, δ = 150.5 (pyridine C-6), 147.6 (pyridine C-2), 147.5 (aniline C-1), 133.7 (pyridine C-4), 131.1 (aniline C-3), 127.7 (aniline C-5), 126.8 (pyridine C-3), 124.4 (pyridine C-5), 116.6 (aniline C-4), 115.7 (aniline C-6), 109.4 (aniline C-2); LC-MS, m/z = 238 [M+1]; calculated for C13H11N5: C, 65.81; H, 4.67; N, 29.52; found: C, 65.80; H, 4.68; N, 29.55.

2-(3-(Pyridin-4-yl)-1H-1,2,4-triazol-5-yl)aniline (2.47): yield: 88.93% (Method A), 91.8% (Method B); mp 261–263 °C; 1H NMR, δ = 6.69–6.52 (m, 3H, H-4, NH2), 6.81 (d, J = 8.2 Hz, 1H, H-6), 7.11 (t, J = 7.8 Hz, 1H, H-5), 7.83–7.70 (d, 1H, H-3), 7.99 (d, J = 5.0 Hz, 2H, pyridine, H-3,5), 8.63 (d, J = 5.1 Hz, 2H, pyridine, H-2,6), 14.35 (s, 1H, NH); 13C NMR, δ = 150.9 (pyridine C-3,5), 147.7 (aniline C-1), 131.4 (aniline C-3), 127.6 (aniline C-5), 120.6 (pyridine C-2,6), 116.8 (aniline C-4), 115.7 (aniline C-6); LC-MS, m/z = 238 [M+1]; calculated for C13H11N5: C, 65.81; H, 4.67; N, 29.52; found: C, 65.78; H, 4.69; N, 29.54.

4-Bromo-2-(3-(pyridin-4-yl)-1H-1,2,4-triazol-5-yl)aniline (2.48): yield: 81.82% (Method A); mp 277–279 °C; 1H NMR, δ = 6.88–6.65 (m, 3H, H-6, NH2), 7.17 (t, J = 8.8 Hz, 1H, H-4), 7.99 (m, 3H, H-3, pyridine, H-3,5), 8.64 (m, 2H, pyridine, H-2.6), 14.50 (s, 1H, NH); LC-MS, m/z = 317 [M+1]; calculated for C13H10BrN5: C, 49.39; H, 3.19; N, 22.15; found: C, 49.44; H, 3.23; N, 22.18.

X-Ray crystallographic analysis of 2-(3-Cyclopropyl-1H-1,2,4-triazol-5-yl)aniline (2.1)

Yellow crystals of compound 2.1 (formula $C_{11}H_{12}N_4$) belong to the orthorhombic system at 173 K with unit cell parameters: a = 9.6093(7), b = 19.1643(12), c = 5.3530(4) Å, volume V = 985.78(12) Å^3, molecular weight Mr = 200.25, Z = 4, space group $Pna2_1$, calculated density dcalc = 1.349 g/cm^3, linear absorption coefficient μ(MoKα) = 0.086 mm^{-1}, and F(000) = 424. A total of 13,137 reflections were collected, of which 1742 were unique (Rint = 0.078), using a Bruker APEX II diffractometer (Billerica, MA, USA) equipped with graphite-monochromated MoKα radiation, a CCD detector, and φ- and ω-scans up to 2Θmax = 50°. The structure was determined by direct methods with the SHELXTL software suite [35]. Hydrogen atoms were identified from difference Fourier maps and refined using a riding model with unconstrained isotropic displacement parameters. Full-matrix least-squares refinement on F^2 was performed in anisotropic mode for non-hydrogen atoms, utilizing all 1742 independent reflections, yielding final agreement factors wR_2 = 0.1053 (R_1 = 0.0511 for 1420 reflections with F > 4σ(F), goodness-of-fit S = 1.094). The complete atomic coordinates and crystallographic parameters for molecule 2.1 have been deposited with the Cambridge Crystallographic Data Centre, 12 Union Road, CB2 1EZ, UK (fax: +44-1223-336033; e-mail: deposit@ccdc.cam.ac.uk) under deposition number CCDC 2352489 and are freely available upon request.

Molecular docking studies

Flexible molecular docking was employed to evaluate the binding affinity of the synthesized molecules toward selected biological targets. The protein structure chosen was DNA gyrase (PDB ID: 2XCT) [36], based on published data concerning the mechanism of antistaphylococcal action [16, 17].

Preparation of ligands

All compounds were sketched in MarvinSketch 20.21.0 and exported in .mol format [37]. Geometry optimization was performed in Chem3D using the MM2 molecular mechanics force field, followed by saving the structures as PDB files. This mechanics-based approach provides reliable geometries for organic molecules owing to its comprehensive parameterization. The resulting PDB files were converted to PDBQT format using AutoDockTools-1.5.6, with default settings retained for the number of rotatable bonds [38].

Preparation of protein target

Protein structures were downloaded from the Protein Data Bank. Unnecessary water molecules and co-crystallized ligands were deleted using Discovery Studio v21.1.0.20298, and the cleaned protein was saved as a PDB file [39]. Polar hydrogen atoms were subsequently added via AutoDockTools-1.5.6, and the file was converted to PDBQT format. Docking was performed with AutoDock Vina using the following grid box parameters: center coordinates (x = −12.436, y = 34.791, z = 67.712) and dimensions (x = 8, y = 8, z = 12) [36]. Binding poses were visualized in Discovery Studio v21.1.0.20298.

To confirm the reliability of the docking protocol, the reference ligand was extracted from the crystal structure, redocked into the active site, and compared with its original conformation [40]. The root-mean-square deviation (RMSD) serves as the standard metric, with values below 2 Å indicating successful reproduction of the experimental pose [41]. The calculated RMSD between the docked and crystallographic ligand conformations was 1.268 Å, determined using the online tool DockRMSD [42]. This result validates the docking procedure as reliable.

Evaluation of antimicrobial activity

Antimicrobial susceptibility of the synthesized compounds was determined according to established protocols [43]. Tests were conducted on Mueller–Hinton agar using a two-fold serial dilution technique in 1 mL volumes, followed by inoculation with 0.1 mL of bacterial suspension (1.5 × 10^8 CFU/mL). The minimal inhibitory concentration (MIC) was recorded as the lowest concentration preventing visible growth in the tube, while the minimal bactericidal concentration (MBC) was defined by the absence of colony growth on agar after subculturing

from clear tubes. Compounds were initially dissolved in DMSO at 1 mg/mL. Preliminary screening employed Staphylococcus aureus ATCC 25923 as the test organism. Culture media and solvent controls were performed in accordance with standard guidelines [43]. To enable direct comparison, MIC and MBC values were converted to micromolar (μM) concentrations accounting for the molecular weight of each derivative. The S. aureus ATCC 25923 strain was sourced from the bacteriological laboratory of the Zaporizhzhia Regional Laboratory Center of the State Sanitary and Epidemiological Service of Ukraine.

SwissADME profiling

Physicochemical properties, pharmacokinetic parameters, and drug-likeness were predicted using the free web-based SwissADME platform. Detailed descriptions of the computational methods and underlying principles of SwissADME are provided in the referenced publications [44-46].

Results and Discussion

Chemical studies

In the course of this research, our focus was on devising a "one-pot" approach for preparing [2-(3-R-1H-[1, 2, 4]-triazol-5-yl)phenyl]amines (2), which could additionally serve as versatile intermediates for constructing novel bioactive heterocyclic systems and evaluating their antistaphylococcal potential. Existing synthetic routes to these compounds are typically multistage [47-49] or rely on the degradative cleavage of triazolo[c]quinazoline frameworks [50]. Seeking an efficient alternative for obtaining novel [2-(3-R-1H-[1,2,4]triazol-5-yl)phenyl]amines (2), we capitalized on the straightforward nature of the Dimroth rearrangement coupled with nucleophilic pyrimidine ring opening in triazolo[c]quinazoline derivatives [51]. Computational modeling of these reaction pathways indicated that acid-catalyzed hydrolysis involving a stoichiometric quantity of water facilitates the Dimroth rearrangement, whereas pyrimidine ring scission requires analogous acid hydrolysis but with excess water [51].

Our initial effort to achieve a "one-pot" preparation of 2-(3-cyclopropyl-1H-1,2,4-triazol-5-yl)-aniline (2.1) proved highly effective **(Scheme 1).** Specifically, acylation of starting material 1.1 with cyclopropanecarbonyl chloride in acetic acid, using sodium acetate as base, afforded the corresponding hydrazide (A) in quantitative yield, which then underwent direct heterocyclization without purification (Method A). The ensuing nucleophilic cleavage of the triazolo[c]quinazoline intermediate (C) necessitated solvent evaporation followed by treatment with an acidified methanol–water mixture (5:1). Under these conditions, target compound 2.1 was isolated in near-quantitative yield (98%). Encouraged by this outcome, we extended the "one-pot" protocol to synthesize analogs 2.2–2.48 **(Scheme 1)**. The optimized procedure incorporates certain adaptations, particularly to address the limited commercial availability of specific acyl halides, which prompted in situ generation of the required acyl chlorides.

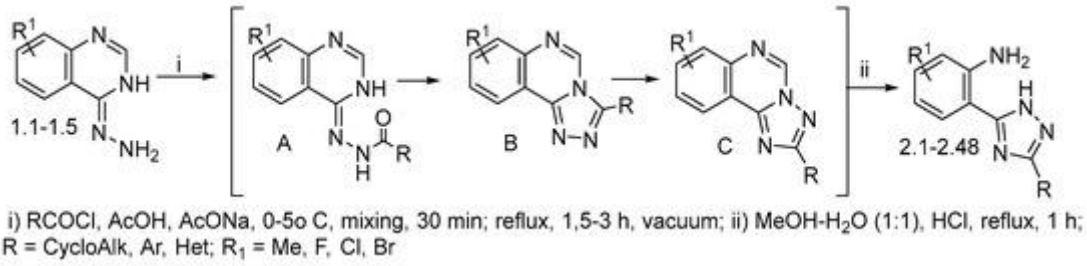

Scheme 1. Preparation of the target compounds 2 employing substituted 4-hydrazinoquinazolines as starting materials.

We also explored an alternative "one-pot" route for accessing compounds 2, utilizing 2-aminobenzonitrile (3.1), (**Scheme 2)** as the precursor. In this approach, the nitrile was initially converted to N'-(2-cyanophenyl)-N,N-dimethylformimidamide (A) through reaction with DMF/DMA. Following removal of excess reagent and solvent, the intermediate was directly subjected to heterocyclization using various carboxylic acid hydrazides in acetic acid (Method B). Subsequent solvent evaporation led to quantitative formation of the triazolo[c]quinazoline framework (C). The final stage mirrored the conditions established in the earlier Method A. Under these optimized conditions, the desired products 2.22–2.27, 2.32, 2.38, 2.46, and 2.47 were obtained in near-quantitative yields.

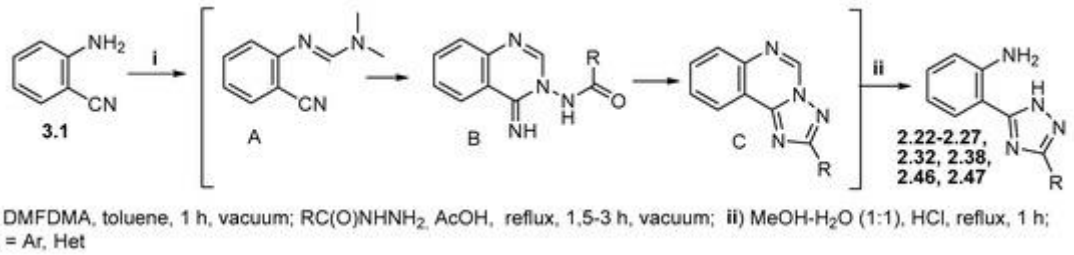

Scheme 2. Preparation of the target compounds 2 employing 2-aminobenzonitriles as starting materials.

The identity and purity of the synthesized compounds were established through a combination of physicochemical techniques, encompassing elemental analysis, LC/MS, ^{1}H and ^{13}C NMR spectroscopy, as well as X-ray crystallography. In the LC-MS spectra of all prepared derivatives, peaks corresponding to the m/z values expected for the proposed molecular formulas were observed.

The conversion to [2-(3-R-1H-[1, 2, 4]-triazol-5-yl)phenyl]amines (2) markedly alters the ^{1}H NMR spectral profile relative to the intermediate [1, 2 ,4]triazolo[1,5-c]quinazolines (C) [52]. Notably, the characteristic low-field singlet (9.70–9.25 ppm) attributable to the proton at the fifth position of the tricyclic framework (C) is absent. Instead, the spectra of compounds 2 display signals for the NH_2 protons of the aniline moiety, appearing as a broad singlet or doublet at 6.72–5.97 ppm (compounds 2.1, 2.2, 2.4–2.6, 2.8–2.14, 2.16–2.18, 2.20–2.23, 2.26, 2.28, 2.30, 2.31, 2.33–2.42, 2.45, 2.46), overlapping as a multiplet with aromatic protons (2.3, 2.7, 2.15, 2.19, 2.24, 2.25, 2.27, 2.29, 2.32, 2.47, 2.48), or entirely missing from the spectrum (2.43, 2.44). The observed broadening or splitting of these amino proton signals is attributable to azole–azole prototropic tautomerism in compounds 2 [32, 50]. Supporting evidence for such tautomeric equilibria includes the broadening, duplication, or disappearance (in 2.24, 2.25, 2.27, 2.32, 2.38, 2.43) of the low-field singlet corresponding to the triazole NH proton. Furthermore, the aromatic protons of the aniline portion in compounds 2 experience an upfield (diamagnetic) shift due to the electron-donating influence of the amino substituent. Additional characteristic signals arise from protons in the substituents at the triazole's third position, with their chemical shifts and multiplicities governed by the substituent's structure [53]. In the ^{13}C NMR spectra, the C1 carbon of the aniline ring exhibits a pronounced downfield (paramagnetic) shift (147.7–141.4 ppm) relative to other aromatic carbons, reflecting the electron-donating effect of the amino group and confirming pyrimidine ring cleavage. The triazole C3 and C5 resonances appear as broad singlets at 162.8–153.7 ppm and 171.5–154.1 ppm (for 2.17, 2.22–2.26) or are undetectable (in 2.1, 2.13, 2.32, 2.46), further indicative of tautomeric processes in DMSO-d_6 solutions.

To definitively validate the “one-pot” preparation of compound 2.1, single-crystal X-ray diffraction analysis was conducted. Crystals suitable for analysis were obtained by slow crystallization from methanol. The triazole ring deviates from coplanarity with the phenyl ring (C11–C6–C5–N2 torsion angle of 16.0(6)°), resulting from competing effects: (1) an intramolecular hydrogen bond N4–H…N2′ (H…N distance 2.02 Å; N–H…N angle 142°) and (2) steric hindrance between the aromatic systems (short intramolecular H7…N1 contact of 2.57 Å, versus the sum of van der Waals radii [54] of 2.67 Å). The amino group adopts a pyramidal geometry, with the sum of valence angles at N4 equaling 328°. The cyclopropyl substituent is oriented such that the C2–H bond is syn-periplanar to the endocyclic C1–N3 bond (N3–C1–C2–H2 torsion angle 11.6°). In the crystalline state, molecules of 2.1 assemble into infinite chains along the crystallographic direction **(Figure 2)** via intermolecular hydrogen bonds N3–H…N1′ (symmetry operation: 0.5+x, 1.5-y, z; H…N distance 2.01 Å; N–H…N angle 172°).

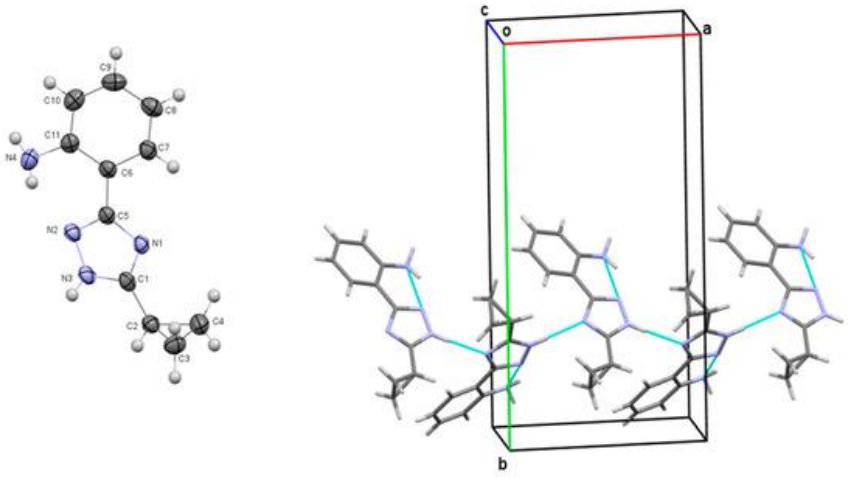

Figure 2. Molecular structure of compound 2.1 as determined by single-crystal X-ray diffraction (thermal ellipsoids for non-hydrogen atoms drawn at the 50% probability level) together with the hydrogen-bonded infinite chain formed by molecules of 2.1 in the crystal packing.

Molecular docking studies

In order to guide subsequent in vitro evaluation of the antistaphylococcal properties of the synthesized compounds and to gain insight into their potential molecular mechanism of action, molecular docking simulations were performed targeting the active site of DNA gyrase. The computed binding affinities (in kcal/mol) and detailed interaction profiles relative to the reference compound Ciprofloxacin are presented in **Table 1**. The results revealed that nearly all investigated ligands—with the exception of compounds 2.17–2.21—exhibited strong binding affinity toward the DNA gyrase inhibitory site, with values spanning −5.6 to −9.2 kcal/mol, in comparison to −6.7 kcal/mol obtained for Ciprofloxacin.

Table 1. The results of studies on the docking of ligand 2 and the native inhibitor to the active site of DNA gyrase (2XCT).

Compound	Affinity (kcal/mol)	Compound	Affinity (kcal/mol)	Compound	Affinity (kcal/mol)
TA *	−6.3	**2.17**	−5.5	**2.34**	−8.1
2.1	−6.7	**2.18**	−5.6	**2.35**	−7.9
2.2	−7.4	**2.19**	−6.1	**2.36**	−8.3
2.3	−8.4	**2.20**	−6.3	**2.37**	−8.3
2.4	−7.1	**2.21**	−6.0	**2.38**	−8.9
2.5	−7.1	**2.22**	−7.9	**2.39**	−8.5
2.6	−7.6	**2.23**	−8.3	**2.40**	−7.9
2.7	−7.4	**2.24**	−8.4	**2.41**	−9.2
2.8	−7.6	**2.25**	−8.0	**2.42**	−8.1
2.9	−7.5	**2.26**	−8.5	**2.43**	−8.6
2.10	−8.6	**2.27**	−8.2	**2.44**	−8.9
2.11	−8.4	**2.28**	−8.6	**2.45**	−8.5
2.12	−7.8	**2.29**	−8.9	**2.46**	−8.0
2.13	−8.1	**2.30**	−8.6	**2.47**	−7.8
2.14	−8.3	**2.31**	−8.7	**2.48**	−8.7
2.15	−7.8	**2.32**	−7.5	**Ciprofloxacin**	−6.7
2.16	−8.1	**2.33**	−7.8	-	-

* TA: (2-(1,2,4-triazol-5-yl)aniline.

As depicted in **Figure 3a**, the reference ligand Ciprofloxacin forms hydrogen bonds involving the carboxylic acid group at position 3 with SER1048 (2.51 Å) and the piperazine NH with ARG458 (3.20 Å), along with a halogen interaction between the fluorine atom and the nucleotide base DC13 (2.85 Å), complemented by van der Waals contacts with nucleotides DG9 (2.96; 3.01; 3.25 Å) and G:DC12 (3.47 Å). Furthermore, the reference ligand engages in multiple hydrophobic interactions, including π–π stacking and π–alkyl contacts with the DNA

nucleotide bases DG8 (4.11; 4.33; 5.05; 5.50 Å), G:DC13 (5.56 Å), and DG9 (3.43; 4.10; 4.18; 4.33 Å), which collectively contribute to its stable positioning within the active site, **(Table 1, Figures 4a and 4b).**

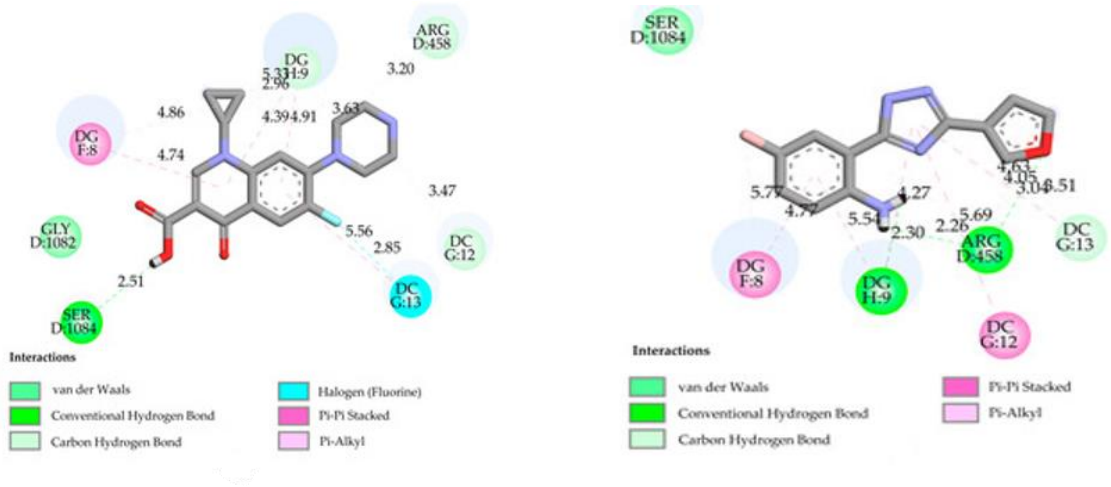

a) b)

Figure 3. Two-dimensional representation of the interactions between the reference compound Ciprofloxacin (a) and the synthesized derivative 2.31 (b) with amino acid residues and DNA nucleotides in the active site of DNA gyrase.

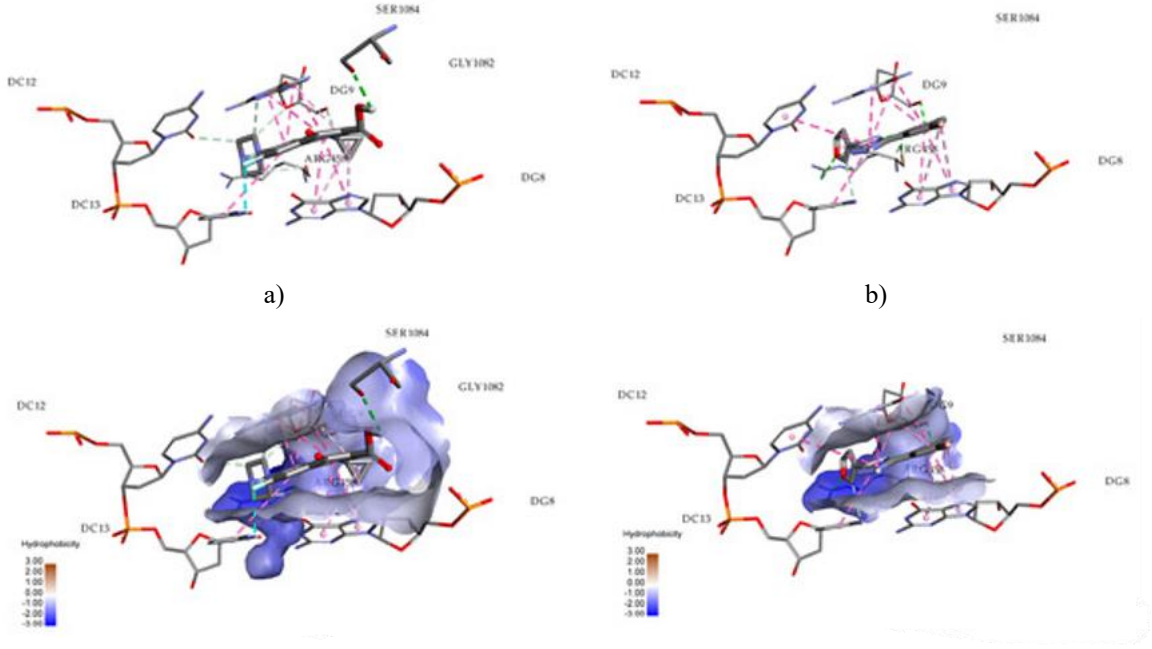

a) b)

c) d)

Figure 4. Three-dimensional conformations illustrating the interactions of Ciprofloxacin (a. b) and compound 2.31 (c, d) with amino acid residues and nucleotides within the active site of DNA gyrase.

The binding poses of the core 2-(1,2,4-triazol-5-yl)aniline moieties across the examined ligands within the active site remain highly consistent, aligning closely with the position occupied by the quinoline ring in the reference compound, **(Figures 3, and 4).** This similarity is likely attributable to the low topological polar surface area, which facilitates a substantial array of comparable interactions with the crystallographically identified amino acids and nucleotides at the binding pocket. A key distinction from Ciprofloxacin is the lack of interaction with SER1048, a residue engaged by the carboxylic acid functionality in the standard ligand.

Conversely, 2-(1,2,4-triazol-5-yl)anilines bearing electron-withdrawing substituents—and consequently displaying elevated affinity—were anchored in the DNA gyrase active site through an expanded network of

hydrogen bonds involving ARG458 and the nucleotide bases (DG8, DG9, DC12, and DC13). For instance **(Figure 3b)**, the robust ligand-receptor complex for compound 2.31 was stabilized by five predicted hydrogen bonds to ARG458 (2.26; 3.04; 3.43 Å), DG9 (2.30 Å), and G:DC13 (3.51 Å), in conjunction with hydrophobic π–π stacking interactions involving DG8 (4.21; 4.36 Å), DG9 (3.74; 4.05; 4.15; 4.71 Å), DC12 (5.69 Å), and DC13 (4.63 Å) **(Figures 4c and 4d).** Additionally, ligand 2.31 features an internal hydrogen bond between N4 and NH_2 (1.85 Å), a feature recurrent in other analogs **(Figure 2)**, that presumably locks the molecule into a more advantageous conformational state.

Overall, the in-depth conformational evaluation of ligands 2—highlighted by 2.31—and Ciprofloxacin, **(Figure 4),** both of which display strong binding affinities, underscores their shared spatial orientations. This supports their capacity to access the hydrophilic cavity of DNA gyrase and establish durable complexes at the active site. These findings suggest a strong likelihood that the developed ligands exert antistaphylococcal effects via DNA gyrase inhibition. To elucidate the structure–activity relationships more thoroughly, all synthesized compounds were advanced to in vitro testing.

Antistaphylococcal activity of synthesized compounds

The antibacterial efficacy of compounds 2 against Staphylococcus aureus ATCC 25923 was assessed **(Table 2)**. The majority of these derivatives demonstrated activity (MIC: 5.2–933.4 μM; MBC: 10.4–933.4 μM). Among the cycloalkyl derivatives (2.1–2.21), compounds 2.1, 2.5, 2.9, 2.12, 2.17, and 2.18 exhibited potent effects, with MIC values ranging from 10.1–438.0 μM and MBCs from 20.2–438.0 μM. Notably, 2.17 and 2.18 displayed the strongest activity in this series (MIC: 10.1–10.6 μM; MBC: 20.2–21.2 μM), approaching that of the benchmark drug Ciprofloxacin (MIC: 4.7 μM; MBC: 9.6 μM). The aryl-substituted analogs (2.22–2.26) also showed efficacy (MIC: 12.4–317.3 μM; MBC: 24.8–786.6 μM), with 2.26 emerging as the standout (MIC: 12.4 μM; MBC: 24.8 μM). In the hetaryl series (2.27–2.48), compounds 2.28–2.31, 2.33–2.35, 2.39, 2.41, and 2.46 displayed robust antistaphylococcal properties (MIC: 5.5–25.6 μM; MBC: 10.4–52.8 μM), whereas the remainder were moderately active (MIC: 42.5–221.0 μM; MBC: 84.9–442.0 μM).

Table 2. Antimicrobial activity of compounds **2** against Staphylococcus aureus ATCC 25923 strain.

Compounds	R^1	R	MBC **, μM	MIC *, μM	MBC/MIC
2.1	H	Cyclopropyl	124.8	62.4	2
2.2	6-Me	Cyclopropyl	933.4	933.4	1
2.3	5-F	Cyclopropyl	916.5	458.2	2
2.4	4-Cl	Cyclopropyl	852.2	852.2	1
2.5	H	Cyclobutyl	23.3	14.6	1.5
2.6	6-Me	Cyclobutyl	876.1	876.1	1
2.7	5-F	Cyclobutyl	861.2	430.6	2
2.8	4-Cl	Cyclobutyl	804.2	402.1	2
2.9	H	Cyclopentyl	438.0	27.4	16
2.10	6-Me	Cyclopentyl	825.4	825.4	1
2.11	5-F	Cyclopentyl	406.0	203.0	2
2.12	4-Cl	Cyclopentyl	47.6	47.6	1
2.13	H	Cyclohexyl	206.3	26.8	7.7
2.14	6-Me	Cyclohexyl	390.1	390.1	1
2.15	5-F	Cyclohexyl	768.3	192.1	4
2.16	4-Cl	Cyclohexyl	723.6	361.3	2
2.17	H	adamantyl-1	21.2	10.6	2
2.18	6-Me	adamantyl-1	20.2	10.1	2
2.19	5-F	adamantyl-1	640.2	320.1	2
2.20	4-Cl	adamantyl-1	608.2	304.1	2
2.21	4-Br	adamantyl-1	535.7	267.9	2
2.22	H	Ph	211.6	26.4	8
2.23	H	4-FC_6H_4	786.6	196.6	4
2.24	H	4-ClC_6H_4	184.6	92.3	2
2.25	H	4-BrC_6H_4	634.6	317.3	2
2.26	H	2-FC_6H_4	24.8	12.4	2
2.27	H	furan-2-yl	442.0	221.0	2

2.28	6-Me	furan-3-yl	52.0	13.0	4
2.29	5-F	furan-3-yl	51.2	25.6	2
2.30	4-Cl	furan-3-yl	23.8	11.9	2
2.31	4-Br	furan-3-yl	10.4	5.2	2
2.32	H	thiophen-2-yl	206.4	103.2	2
2.33	5-F	thiophen-2-yl	48.0	24.0	2
2.34	6-Me	thiophen-3-yl	12.2	12.2	1
2.35	5-F	thiophen-3-yl	48.0	6.1	8
2.36	4-Cl	thiophen-3-yl	180.8	45.2	4
2.37	4-Br	thiophen-3-yl	311.3	77.8	4
2.38	H	benzofuran-2-yl	361.8	180.9	2
2.39	6-Me	benzofuran-2-yl	21.4	10.7	2
2.40	5-F	benzofuran-2-yl	84.9	42.5	2
2.41	4-Cl	benzofuran-2-yl	40.2	20.1	2
2.42	4-Br	benzofuran-2-yl	140.7	140.7	1
2.43	H	benzothiophen-2-yl	342.0	171.0	2
2.44	H	indol-2-yl	363.2	181.6	2
2.45	H	pyridin-2-yl	210.6	105.3	2
2.46	H	pyridin-3-yl	52.8	13.2	4
2.47	H	pyridin-4-yl	210.6	105.3	2
2.48	Br	pyridin-4-yl	158.2	79.1	2
Ciprofloxacin			9.6	4.7	2

* MIC—minimal inhibitory concentration; ** MBC—minimum bactericidal concentration.

The most potent compounds identified against the S. aureus strain were 5-bromo-2-(3-(furan-3-yl)-1H-1,2,4-triazol-5-yl)aniline (2.31) and 5-fluoro-2-(3-(thiophen-3-yl)-1H-1,2,4-triazol-5-yl)aniline (2.35), exhibiting MIC values of 5.2 μM and 6.1 μM, respectively, and thus closely approaching the activity of the reference agent Ciprofloxacin **(Table 2)**. Furthermore, evaluation of the MBC/MIC ratios **(Table 2)** revealed that nearly all compounds (with the exceptions of 2.9 and 2.13) displayed bactericidal rather than bacteriostatic behavior, conferring a clear therapeutic advantage.

SAR analysis

Integrating the molecular docking outcomes with the in vitro antibacterial data against S. aureus **(Table 2)**, the structure–activity relationships can be summarized as follows:

- Incorporation of a cyclopropane substituent at the triazole's third position in the parent 2-(1H-1,2,4-triazol-5-yl) aniline scaffold imparts measurable antistaphylococcal activity. Expanding the cycloalkyl ring by additional methylene units generally improves potency, while introduction of the adamantyl pharmacophore yields particularly strong effects. In contrast, halogen substitution on the aniline ring almost uniformly diminishes or abolishes activity in this subclass;
- Substitution of the cycloalkyl group with a phenyl ring at the triazole's third position preserves antistaphylococcal efficacy. However, halogenation of this phenyl ring tends to reduce activity, whereas repositioning a fluorine atom to the ortho position markedly enhances it;
- Attachment of five- or six-membered heterocyclic moieties containing electron-donating heteroatoms (O, N, S) at the triazole's third position consistently confers potent antistaphylococcal properties. This enhancement correlates with strengthened π–electron interactions with DNA nucleotides, resulting in closer mimicry of the binding pose within the enzyme's active site. Addition of a methyl group to the aniline ring further boosts activity. Notably, unlike the cycloalkyl series, halogen substitution on the aniline portion in hetaryl-substituted analogs reliably increases potency.

Overall, the observed antistaphylococcal effects arise from structural elements that promote favorable interactions with the DNA gyrase active site. The hydrogen-bonding profile of the 2-(1,2,4-triazol-5-yl)aniline core closely resembles that of Ciprofloxacin. The absence of a carboxylic acid moiety in the synthesized ligands is offset by electron-withdrawing substituents at the third and para (or meta) positions of the scaffold.

SwissADME analysis

The principle of "drug-likeness" is fundamental to modern drug discovery, providing essential filters in early-stage development that improve the likelihood of clinical success [55]. These parameters profoundly influence key pharmacokinetic attributes—absorption, distribution, metabolism, and excretion—ultimately determining the therapeutic potential and efficacy of candidate molecules. Drug-likeness profiles for the most active compounds (2.17, 2.18, 2.26, 2.28, 2.30, 2.31, 2.34, 2.35, 2.39, 2.46) alongside the reference Ciprofloxacin are compiled in **Table 3**.

Table 3. Physicochemical descriptors and pharmacokinetic properties of compounds **2** provided by SwissADME.

Physicochemical Descriptors and Predicted Pharmacokinetic Properties *	Compounds										
	2.17	**2.18**	**2.26**	**2.28**	**2.30**	**2.31**	**2.34**	**2.35**	**2.39**	**2.46**	**CF ****
MW (Da) (<500)	294.39	308.42	252.27	240.26	260.68	305.13	256.33	260.29	290.32	237.26	331.34
n-ROTB (<10)	2	2	2	2	2	2	2	2	2	2	3
n-HBA (<10)	2	2	2	3	3	3	2	3	3	3	5
n-HBD (≤5)	2	2	2	2	2	2	2	2	2	3	2
TPSA (<140, Å²)	67.59	67.59	87.82	80.73	80.73	80.73	95.83	95.83	80.73	80.48	74.57
logP (≤5)	3.21	3.54	2.05	2.06	2.30	2.34	2.74	2.69	3.07	1.66	1.10
Molar refractivity	88.11	93.08	73.68	68.89	68.94	71.63	74.50	69.49	86.40	69.45	95.25
Gastrointestinal absorption	high	high	high	High	high	high	high	high	high	high	high
Drug-likeness											
Lipinski (Pfizer) filter [43]	yes	yes	yes	Yes	yes	yes	yes	yes	yes	yes	yes
Veber (GSK) filter [44]	yes	yes	yes	Yes	yes	yes	yes	yes	yes	yes	yes
Muegge (Bayer) filter [45]	yes	yes	yes	Yes	yes	yes	yes	yes	yes	yes	yes
Ghose filter [46]	yes	yes	yes	Yes	yes	yes	yes	yes	yes	yes	yes
Egan filter [47]	yes	yes	yes	Yes	yes	yes	yes	yes	yes	yes	yes
Bioavailability score [48]	0.55	0.55	0.55	0.55	0.55	0.55	0.55	0.55	0.55	0.55	0.55
Lead-likeness	no	no	yes	No	yes	yes	yes	yes	yes	no	yes

* MW= molecular weight; n-ROTB= number of rotatable bonds; n-HBA= number of hydrogen bond acceptors; n-HBD= number of hydrogen bond donors; TPSA= topological polar surface area; ** CF= Ciprofloxacin.

The virtual screening outcomes revealed that the tested compounds, along with the standard antibiotic Ciprofloxacin, satisfied the essential "drug-like" properties based on key parameters: molecular weight (MW in Da) below 500, number of hydrogen bond acceptors (n-HBA) under 10, number of hydrogen bond donors (n-HBD) no more than 5, and topological polar surface area (TPSA) less than 140 Å². The acceptable TPSA values (below 140 Å²) are strongly linked to efficient passive diffusion through cell membranes, suggesting that these

molecules possess strong potential for crossing the blood–brain barrier and engaging effectively with biological targets. Among the evaluated substances, Ciprofloxacin displayed the lowest LogP value. Compound 2.46 exhibited a LogP close to that of Ciprofloxacin, likely due to the incorporation of a pyridine ring. In contrast, the remaining compounds showed greater lipophilicity compared to Ciprofloxacin, with particularly elevated LogP values observed in those containing adamantane groups. The structures also performed well in bioavailability predictions [56], achieving a score of 0.55. Additionally, the molecules were assessed against five widely used drug-likeness rules (Lipinski, Veber, Muegge, Ghose, and Egan) [57-61] that are routinely applied in the pharmaceutical industry to improve the quality of compound libraries. The computed physicochemical properties generally indicated compliance with these rules in nearly all cases, with minimal violations. Overall, most of the compounds exhibited strong drug-like characteristics and appear promising for additional structural refinement. Therefore, the favorable outcomes from the SwissADME evaluation support further modifications of the most potential candidates in this series to optimize their properties.

Conclusion

The present study describes an efficient “one-pot” synthetic route to 48 derivatives of [2-(3-R-1H-[1, 2, 4]triazol-5-yl)phenyl]amines, achieved through regioselective transformation of either substituted 4-hydrazinoquinazolines or 2-aminobenzonitriles with appropriate carboxylic acid derivatives. The reactions proceeded with high reproducibility and excellent yields. Combined in silico and in vitro screening identified several compounds as potent antibacterial agents against S. aureus ATCC 25923, displaying activity comparable to or better than the reference drug Ciprofloxacin. Antibacterial potency was found to depend strongly on the nature of the substituent at the 3-position of the 1,2,4-triazole ring as well as modifications on the aniline moiety, highlighting the need for further structure–activity relationship investigations within this chemical series. Overall, the synthesized [2-(3-R-1H-[1, 2, 4]triazol-5-yl)phenyl]amines represent a promising scaffold warranting additional structural optimization and in-depth evaluation as potential antistaphylococcal agents. Expanded testing against both standard and clinically relevant MRSA strains is expected to further clarify and enhance their therapeutic potential.

Acknowledgments: None

Conflict of Interest: None

Financial Support: None

Ethics Statement: None

References

1. El-Aleam, R.H.A.; George, R.F.; Georgey, H.H.; Abdel-Rahman, H.M. Bacterial virulence factors: A target for heterocyclic compounds to combat bacterial resistance. RSC Adv. 2021, 11, 36459–82.
2. Koulenti, D.; Xu, E.; Mok, I.Y.S.; Song, A.; Karageorgopoulos, D.E.; Armaganidis, A.; Lipman, J.; Tsiodras, S. Novel Antibiotics for Multidrug-Resistant Gram-Positive Microorganisms. Microorganisms 2019, 7, 270.
3. Theuretzbacher, U. Resistance drives antibacterial drug development. Curr. Opin. Pharmacol. 2011, 11, 433–8.
4. Vimalah, V.; Getha, K.; Mohamad, Z.N.; Mazlyzam, A.L. A Review on Antistaphylococcal Secondary Metabolites from Basidiomycetes. Molecules 2020, 25, 5848.
5. Brown, E.; Wright, G. Antibacterial drug discovery in the resistance era. Nature 2016, 529, 336–43.
6. Esposito, S.; Blasi, F.; Curtis, N.; Kaplan, S.; Lazzarotto, T.; Meschiari, M.; Mussini, C.; Peghin, M.; Rodrigo, C.; Vena, A.; et al. New Antibiotics for Staphylococcus aureus Infection: An Update from the World Association of Infectious Diseases and Immunological Disorders (WAidid) and the Italian Society of Anti-Infective Therapy (SITA). Antibiotics 2023, 12, 742.
7. Wright, P.M.; Seiple, I.B.; Myers, A.G. The evolving role of chemical synthesis in antibacterial drug discovery. Angew. Chem. Int. Ed. 2014, 53, 8840–69.
8. Doytchinova, I. Drug Design-Past, Present, Future. Molecules 2022, 27, 1496.

9. Anstead, G.M.; Cadena, J.; Javeri, H. Treatment of infections due to resistant Staphylococcus aureus. Methods Mol. Biol. 2014, 1085, 259–309.
10. Bisacchi, G.S.; Manchester, J.I. A New-Class Antibacterial–Almost. Lessons in Drug Discovery and Development: A Critical Analysis of More than 50 Years of Effort toward ATPase Inhibitors of DNA Gyrase and Topoisomerase IV. ACS Infect. Dis. 2015, 1, 4–41.
11. Khan, T.; Sankhe, K.; Suvarna, V.; Sherje, A.; Patel, K.; Dravyakar, B. DNA gyrase inhibitors: Progress and synthesis of potent compounds as antibacterial agents. Biomed. Pharmacother. 2018, 103, 923–38.
12. Durcik, M.; Tomašič, T.; Zidar, N.; Zega, A.; Kikelj, D.; Mašič, L.P.; Ilaš, J. ATP-competitive DNA gyrase and topoisomerase IV inhibitors as antibacterial agents. Expert Opin. Ther. Pat. 2019, 29, 171–80.
13. Dighe, S.N.; Collet, T.A. Recent advances in DNA gyrase-targeted antimicrobial agents. Eur. J. Med. Chem. 2020, 199, 112326.
14. Man, R.-J.; Zhang, X.-P.; Yang, Y.-S.; Jiang, A.-Q.; Zhu, H.-L. Recent Progress in Small Molecular Inhibitors of DNA Gyrase. Curr. Med. Chem. 2021, 28, 5808–30.
15. Poonam, P.; Ajay, K.; Akanksha, K.; Tamanna, V.; Vritti, P. Recent Development of DNA Gyrase Inhibitors: An Update. Mini-Rev. Med. Chem. 2024, 24, 1001–1030.
16. Ashley, R.E.; Dittmore, A.; McPherson, S.A.; Turnbough, C.L., Jr.; Neuman, K.C.; Osheroff, N. Activities of gyrase and topoisomerase IV on positively supercoiled DNA. Nucleic Acids Res. 2017, 45, 9611–24.
17. Hiasa, H. DNA Topoisomerases as Targets for Antibacterial Agents. Methods Mol. Biol. 2018, 1703, 47–62.
18. Watkins, R.R.; Thapaliya, D.; Lemonovich, T.L.; Bonomo, R.A. Gepotidacin: A novel, oral, 'first-in-class' triazaacenaphthylene antibiotic for the treatment of uncomplicated urinary tract infections and urogenital gonorrhoea. J. Antimicrob. Chemother. 2023, 78, 1137–42.
19. Terreni, M.; Taccani, M.; Pregnolato, M. New Antibiotics for Multidrug-Resistant Bacterial Strains: Latest Research Developments and Future Perspectives. Molecules 2021, 26, 2671.
20. Naeem, A.; Badshah, S.L.; Muska, M.; Ahmad, N.; Khan, K. The Current Case of Quinolones: Synthetic Approaches and Antibacterial Activity. Molecules 2016, 21, 268.
21. Millanao, A.R.; Mora, A.Y.; Villagra, N.A.; Bucarey, S.A.; Hidalgo, A.A. Biological Effects of Quinolones: A Family of Broad-Spectrum Antimicrobial Agents. Molecules 2021, 26, 7153.
22. Fesatidou, M.; Anthi, P.; Geronikaki, A. Heterocycle Compounds with Antimicrobial Activity. Curr. Pharm. Des. 2020, 26, 867–904.
23. Murugaiyan, J.; Kumar, P.A.; Rao, G.S.; Iskandar, K.; Hawser, S.; Hays, J.P.; Mohsen, Y.; Adukkadukkam, S.; Awuah, W.A.; Jose, R.A.M.; et al. Progress in Alternative Strategies to Combat Antimicrobial Resistance: Focus on Antibiotics. Antibiotics 2022, 11, 200.
24. Boparai, J.K.; Sharma, P.K. Mini Review on Antimicrobial Peptides, Sources, Mechanism and Recent Applications. Protein Pept. Lett. 2020, 27, 4–16.
25. Nasiri Sovari, S.; Zobi, F. Recent Studies on the Antimicrobial Activity of Transition Metal Complexes of Groups 6–12. Chemistry 2020, 2, 418–52.
26. Feng, G.; Tengfei, W.; Jiaqi, X.; Gang, H. Antibacterial activity study of 1,2,4-triazole derivatives. Eur. J. Med. Chem. 2019, 173, 274–81.
27. Strzelecka, M.; Świątek, P. 1,2,4-Triazoles as Important Antibacterial Agents. Pharmaceuticals 2021, 14, 224.
28. Kazeminejad, Z.; Marzi, M.; Shiroudi, A.; Kouhpayeh, S.A.; Farjam, M.; Zarenezhad, E. Novel 1,2,4-Triazoles as Antifungal Agents. Biomed. Res. Int. 2022, 22, 4584846.
29. Xuemei, G.; Zhi, X. 1,2,4-Triazole hybrids with potential antibacterial activity against methicillin-resistant Staphylococcus aureus. Arch. Pharm. 2020, 354, e2000223.
30. Jie, L.; Junwei, Z. The Antibacterial Activity of 1,2,3-triazole- and 1,2,4-Triazole-containing Hybrids against Staphylococcus aureus: An Updated Review (2020–Present). Curr. Top. Med. Chem. 2022, 22, 41–63.
31. Verdirosa, F.; Gavara, L.; Sevaille, L.; Tassone, G.; Corsica, G.; Legru, A.; Feller, G.; Chelini, G.; Mercuri, P.S.; Tanfoni, S.; et al. 1,2,4-Triazole-3-Thione Analogues with a 2-Ethylbenzoic Acid at Position 4 as VIM-type Metallo-β-Lactamase Inhibitors. ChemMedChem 2022, 17, e202100699.
32. Sergeieva, T.; Bilichenko, M.; Kholodnyak, S.; Monaykina, Y.; Okovytyy, S.; Kovalenko, S.; Voronkov, E.; Leszczynski, J. Origin of Substituent Effect on Tautomeric Behavior of 1,2,4-Triazole Derivatives. Combined Spectroscopic and Theoretical Study. J. Phys. Chem. A 2016, 120, 10116–22.

33. Pylypenko, O.O.; Okovytyy, S.I.; Sviatenko, L.K.; Voronkov, E.O.; Shabelnyk, K.P.; Kovalenko, S.I. Tautomeric behavior of 1,2,4-triazole derivatives: Combined spectroscopic and theoretical study. Struct. Chem. 2023, 34, 181–92.
34. Zhang, Y.; Chen, L.; Xu, H.; Li, X.; Zhao, L.; Wang, W.; Li, B.; Zhang, X. 6,7-Dimorpholinoalkoxy quinazoline derivatives as potent EGFR inhibitors with enhanced antiproliferative activities against tumor cells. Eur. J. Med. Chem. 2018, 147, 77–89.
35. Sheldrick, G.M. A Short History of SHELX. Acta Crystallogr. 2008, A64, 112–22.
36. Kumar, H.S.S.; Kumar, S.R.; Kumar, N.N.; Ajith, S. Molecular docking studies of gyrase inhibitors: Weighing earlier screening bedrock. In Silico Pharmacol. 2021, 9, 2.
37. MarvinSketch version 20.21.0, ChemAxon. Available online: http://www.chemaxon.com (accessed on 20 December 2023).
38. Trott, O.; Olson, A.J. AutoDock Vina: Improving the speed and accuracy of docking with a new scoring function, efficient optimization, and multithreading. J. Comput. Chem. 2010, 31, 455–61.
39. Discovery Studio Visualizer v21.1.0.20298. Accelrys Software Inc. Available online: https://www.3dsbiovia.com (accessed on 20 December 2023).
40. Baber, J.C.; Thompson, D.C.; Cross, J.B.; Humblet, C. GARD: A Generally Applicable Replacement for RMSD. J. Chem. Inf. Model. 2009, 49, 1889–900.
41. Warren, G.L.; Andrews, C.W.; Capelli, A.-M.; Clarke, B.; LaLonde, J.; Lambert, M.H.; Lindvall, M.; Nevins, N.; Semus, S.F.; Senger, S.; et al. A critical assessment of docking programs and scoring functions. J. Med. Chem. 2005, 49, 5912–31.
42. DockRMSD. Docking Pose Distance Calculation. 2022. Available online: https://zhanggroup.org/DockRMSD/ (accessed on 23 January 2024).
43. CLSI. Performance Standards for Antimicrobial Susceptibility Testing, 30th ed.; Wayne, P.A., Ed.; CLSI Supplement M100; Clinical and Laboratory Standards Institute: Malvern, PA, USA, 2020; ISBN 978-1-68440-066-9 [Print]; ISBN 978-1-68440-067-6 [Electronic].
44. SwissADME. Available online: http://www.swissadme.ch/index.php# (accessed on 27 October 2023).
45. Bilyi, A.K.; Antypenko, L.M.; Ivchuk, V.V.; Kamyshnyi, O.M.; Polishchuk, N.M.; Kovalenko, S.I. 2-Heteroaryl-[1,2,4]triazolo[1,5-c]quinazoline-5(6 H)-thiones and Their S-Substituted Derivatives: Synthesis, Spectroscopic Data, and Biological Activity. ChemPlusChem 2015, 80, 980–9.
46. Nosulenko, I.S.; Voskoboynik, O.Y.; Berest, G.G.; Safronyuk, S.L.; Kovalenko, S.I.; Kamyshnyi, O.M.; Polishchuk, N.M.; Sinyak, R.S.; Katsev, A.V. Synthesis and Antimicrobial Activity of 6-Thioxo-6,7-dihydro-2H-[1,2,4]triazino[2,3-c]-quinazolin-2-one Derivatives. Sci. Pharm. 2014, 82, 483–500.
47. Francis, J.E.; Cash, W.D.; Psychoyos, S.; Ghai, G.; Wenk, P.; Friedmann, R.C.; Atkins, C.; Warren, V.; Furness, P.; Hyun, J.L.; et al. Structure-activity profile of a series of novel triazoloquinazoline adenosine antagonists. J. Med. Chem. 1988, 31, 1014–20.
48. Balo, C.; López, C.; Brea, J.M.; Fernánde, F.; Caamaño, O. Synthesis and Evaluation of Adenosine Antagonist Activity of a Series of [1,2,4]Triazolo[1,5-c]quinazolines. Chem. Pharm. Bull. 2007, 55, 3725.
49. Khan, G.; Sreenivasa, S.; Govindaiah, S.; Chandramohan, V.; Shetty, P.R. Synthesis, biological screening, in silico study and fingerprint applications of novel 1,2,4-triazole derivatives. J. Het. Chem. 2020, 57, 2010–23.
50. Kholodnyak, S.V.; Schabelnyk, K.P.; Zhernova, G.O.; Sergeieva, T.Y.; Ivchuk, V.V.; Voskoboynik, O.Y.; Kovalenko, S.I.; Trzhetsinskii, S.D.; Okovytyy, S.I.; Shishkina, S.V. Hydrolytic cleavage of pyrimidine ring in 2-aryl-[1,2,4]triazolo[1,5-c]-quinazolines: Physico-chemical properties and hypoglycemia activity of the synthesized compounds. News Pharm. 2015, 3, 9–17.
51. Pylypenko, O.O.; Sviatenko, L.K.; Shabelnyk, K.P.; Kovalenko, S.I.; Okovytyy, S.I. Synthesis and hydrolytic decomposition of 2-hetaryl[1,2,4]triazolo[1,5-c]quinazolines: DFT Study. Struct. Chem. 2024, 35, 97–104.
52. Kovalenko, S.I.; Antypenko, L.M.; Bilyi, A.K.; Kholodnyak, S.V.; Karpenko, O.V.; Antypenko, O.M.; Mykhaylova, N.S.; Los, T.I.; Kolomoets, O.S. Synthesis and Anticancer Activity of 2-(Alkyl-, Alkaryl-, Aryl-, Hetaryl-)-[1,2,4]triazolo[1,5-c]quinazolines. Sci. Pharm. 2013, 81, 359–91.
53. Breitmaier, E. Structure Elucidation by NMR in Organic Chemistry: A Practical Guide, 3rd ed.; Wiley: Hoboken, NJ, USA, 2002; 270p, ISBN 978-0-470-85007-7.

54. Zefirov, Y.V. Reduced intermolecular contacts and specific interactions in molecular crystals. Crystallogr. Rep. 1997, 42, 865–886. Available online: https://inis.iaea.org/search/searchsinglerecord.aspx?recordsFor=SingleRecord&RN=30003683 (accessed on 10 March 2024).
55. Tao, L.; Zhang, P.; Qin, C.; Chen, S.Y.; Zhang, C.; Chen, Z.; Zhu, F.; Yang, S.Y.; Wei, Y.Q.; Chen, Y.Z. Recent progresses in the exploration of machine learning methods as in-silico ADME prediction tools. Adv. Drug Deliv. Rev. 2015, 86, 83–100.
56. Martin, Y.C. A bioavailability score. J. Med. Chem. 2005, 48, 3164–70.
57. Lipinski, C.A.; Lombardo, F.; Dominy, B.W.; Feeney, P.J. Experimental and computational approaches to estimate solubility and permeability in drug discovery and development settings. Adv. Drug Deliv. Rev. 2001, 46, 3–26.
58. Veber, D.F.; Johnson, S.R.; Cheng, H.-Y.; Smith, B.R.; Ward, K.W.; Kopple, K.D. Molecular properties that influence the oral bioavailability of drug candidates. J. Med. Chem. 2002, 45, 2615–23.
59. Muegge, I.; Heald, S.L.; Brittelli, D. Simple selection criteria for drug-like chemical matter. J. Med. Chem. 2001, 44, 1841–6.
60. Ghose, A.K.; Viswanadhan, V.N.; Wendoloski, J.J. A knowledge-based approach in designing combinatorial or medicinal chemistry libraries for drug discovery. 1. A qualitative and quantitative characterization of known drug databases. J. Combin. Chem. 1999, 1, 55–68.
61. Egan, W.J.; Merz, K.M.; Baldwin, J.J. Prediction of drug absorption using multivariate statistics. J. Med. Chem. 2000, 43, 3867–77.